Synergic coordination of stem cells is required to induce a regenerative response in anthozoan cnidarians

Aldine Amiel, Kevin Foucher, Solène Ferreira, Eric Röttinger

Synergic coordination of stem cells is required to induce a regenerative response in anthozoan cnidarians

Aldine R. Amiel, Kevin Foucher, Solène Ferreira, Eric Röttinger*

Université Côte d'Azur, CNRS, INSERM, Institute for Research on Cancer and Aging (IRCAN), Nice, France

Email addresses:

aldine.amiel@unice.fr, kevin.foucher@unice.fr solene.ferreira.ca@gmail.com, eric.rottinger@unice.fr

* Please direct correspondence to:

Eric Röttinger

T: +33 (0)4 93 37 77 91

E: eric.rottinger@unice.fr

Abstract

Little is known about the origin of the inductive signal that translates the amputation stress into a cooperative cellular response. By studying the process underlying the reformation of lost body parts in the anthozoan cnidarian *Nematostella vectensis*, we identified a regeneration-inducing structure that, via a tissue crosstalk, is responsible for the initiation of the repair program. We further revealed for the first time in anthozoan cnidarians, that fast and slow-cycling/quiescent stem cells respond to the amputation stress and actively participate in the reformation of lost body parts. Importantly, a synergic interaction of both stem cell populations is required to complete the regeneration process. Our findings suggest that the emergence/loss of structure complexity/compartmentalization influences the proprieties of tissue plasticity, changes the competence of a tissue to reprogram and, in the context of regeneration, the capacity of the tissue to emit or respond to a regeneration-inducing signal.

Keywords: Whole body regeneration, Tissue repair, Tissue crosstalk, Label retaining cells, Stem cells, Cnidarian, Anthozoan, Sea anemone, *Nematostella vectensis*,

Background

The process of regeneration is the re-formation of damaged or missing body parts that in bilaterian animals, involves cellular migration and proliferation of adult stem cells or de-differentiated cell populations. In combination with the remodeling of existing cells/tissues, these cellular processes are crucial to re-establish the symmetry and the proportion of the body [1]. Regeneration is widespread among metazoans and has fascinated scientists for centuries [2,3]. Still, our understanding of why some animals regenerate while others can't remains largely unknown. In the past 10 years, historical invertebrate whole-body regeneration models such as Planaria and Cnidaria have re-emerged and are taking advantage of modern cellular and molecular techniques to understand the complex process of regeneration [4-7]. Important insight has been gained from these species that have increased our understanding about the cellular and molecular mechanisms underlying regeneration. Yet little is known about how the organism translates the amputation stress into a regeneration inducing signal and the origin as well as the nature of the inductive signal required for the cooperation of cell populations during the regeneration process.

The level of regenerative abilities varies across the animal kingdom [7]. While vertebrates can regenerate certain structures and tissues, planarians and cnidarians posses extraordinary whole-body regeneration capacities and can regrow missing body parts when dissected into small pieces [2,8]. Nonetheless, their regenerative capacities have limitation at both the species and also the tissues level. For instance in planarians, isolation of the most anterior part of its body (region in front of the photoreceptor) or the

pharynx does not lead to regeneration as these regions are devoid of planarian specific pluripotent stem cells, the neoblasts [9-11]. In *Hydra*, the isolated body column, named gastric region, possesses the ability to regenerate while the isolated head, pedal disk or tentacles cannot. The absence of regeneration from these isolated parts is due to the lack of hydrozoan specific pluripotent stem cells, the i-cells (interstitial stem cells), in these highly differentiated and specialized regions of the body [12,13]. Thus, identifying the regenerative limits of a given organism and using them for experimental approaches has led to important findings on the location of stem cell populations and their dynamics during the complex biological process of regeneration.

To date, the majority of studies addressing the role of stem cells during regeneration in cnidarians were performed using Hydrozoa such as *Hydra* and *Hydractinia* [2,14-17]. While *Hydra* is well known to have developed an alternative mechanism to regenerate a head in a stem-cell (i-cell) depleted context [18], those classically considered fast cycling i-cells are under "normal" conditions involved in the regeneration process in *Hydra* and *Hydractinia* [1,19-23]). Only recently, a study in *Hydra* has described slow cycling cells that are part of the pluripotent i-cell as well as the unipotent epithelial stem cell populations and involved in regeneration [24]. However, nothing is known about the relationship between fast and slow cycling stem cells, their hierarchy and how they are interacting to trigger tissue reprograming for regeneration. This question remains unanswered not only in hydrozoans, but in cnidarians in general.

Cnidarians are composed of two major groups, the Anthozoa (coral, sea anemone) and the Medusozoa, that include Hydrozoa, Schyphozoa and Cubozoa [25-30]. Interestingly, the crown-group cnidarians (the living representatives) are genetically as divergent as protostomes and deuterostomes [31,32] and it has been proposed that none of the cnidarian clades is representing the entire group [32]. Thus, it is of great interest to compare the regenerative strategies between hydrozoan and non-hydrozoan cnidarians in order to understand the similarities/differences and evolution of the cellular and molecular mechanisms driving regeneration. Importantly, the presence of adult stem cells has yet to be discovered in non-hydrozoan cnidarians.

Anthozoa diverged early within the cnidarian phylogeny [29,33] and form the largest group of cnidarian [34,35] that display anatomical differences compared to other cnidarian polyps. Exclusively anthozoans possess mesenteries that are well-defined anatomical structures located in the gastric cavity, fulfilling the digestive and sexual reproduction roles of the individual polyp. Mesenteries are multifunctional tissues of combined ectodermal and endodermal origins that in addition to the germ lineage and digestive cells also possesses various additional cell types such as muscle cells and cnidocytes (stinging cells) [36-38]. Because of its i) phylogenetic position, the ii) ease to control spawning and fertilization [39-41] and thus the access to embryonic, larval and post-metamorphic stages all year round, iii) a sequenced genome [42] as well as iv) available cellular and molecular tools for functional genomics [43,44] and genome editing [45], the anthozoan sea anemone *Nematostella vectensis* has become a leading model to gain new insight into animal evolution [42,46,47] and early cnidarian

development [48-55]. *Nematostella* possesses also high regenerative abilities and therefore is a potent model to better understand the relationship between embryonic development and regeneration [44,56]. However, our knowledge concerning the morphological, cellular and molecular mechanisms underlying whole body regeneration in *Nematostella* is still in its early phase [57-61]. Recent work has begun to describe the morphological and cellular events involved in the regeneration process in *Nematostella* [59,60,62]. Wound healing after head amputation is already completed within six hours post amputation (hpa) and oral regeneration following sub-pharyngeal amputation occurs in stereotypic steps [62]. This process is first visible when the most oral part of the remaining mesenteries fuses together and enters in contact with the epithelia at the amputation site. The most oral part of the mesenteries is at the origin of the internal part of the pharynx that completes its regeneration at the same time than the tentacles bulbs form and elongate [62]. The various stages of the polyp's life are defined by clear morphological characteristics (i.e. number of tentacles and mesenteries, presence of gametes) and cell proliferation is necessary for oral regeneration in juveniles [59] as well as in adults [62]. Nonetheless, in juvenile as well as in adult *Nematostella*, the first morphogenetic step of regeneration is proliferation independent and only later steps require mitotic activity to fully complete oral regeneration following sub-pharyngeal amputation [62]. While this study laid down a foundation for functional work on anthozoan regeneration, basic but crucial questions about the regenerative capacities in *Nematostella* still remain unanswered: i) are there any body part, tissue and/or age specific limits of its regenerative abilities? ii) what is the cellular/tissue origin of the signal(s) that initiates cell proliferation and/or regeneration? iii) what are the cellular

mechanisms underlying this phenomenon, and importantly, iv) are there adult stem cells in anthozoans and v) are they involved in the regeneration process?

In the present study we combined classical grafting experiments with cellular approaches to address these questions. This strategy enabled us to highlight a crucial crosstalk between the mesenteries and the surrounding epithelia of the body wall required for regeneration and to identify that the mesenteries are crucial to induce proliferation/regeneration in *Nematostella*. We further identified at least two cell populations, a fast cycling one and a quiescent/slow cycling one that are required in a combinatorial manner to trigger a regenerative response. Both of these cell populations are re-activated in response to the amputation stress and participate in the regeneration process. Importantly, our work provides the first set of evidences for the existence of at least two adult stem cell populations in anthozoans that synergize to drive efficient regeneration in the anthozoan cnidarian *Nematostella*.

Materials and methods

Animal culture

Nematostella vectensis were cultivated at the Institute for Research on Cancer and Aging, Nice (IRCAN) of the University of Nice. Adult and juvenile animals were cultured in 1/3X ASW (Artificial seawater, Tropic-Marin Bio-actif system sea salt) and maintained at 17°C or 22°C for adults and juveniles, respectively. Adults were fed five times a week with freshly hatched artemia. Spawning to obtain juveniles was carried out as described in [39]. Juveniles for cutting experiments were raised until six weeks after fertilization. Starting 2 weeks post fertilization, they were feed once a week with 1ml of smashed artemia during four weeks.

Cutting, tissue isolation and grafting experiments

Juveniles or adults were relaxed by adding 1 ml of 7.14% $MgCl_2$ in 5ml 1/3 ASW and left on a light table during 10 to 15 min until they were relaxed enough for surgical interventions. Polyps were cut using a microsurgery scalpel (Swann-Morton, n°15). Each cut was performed perpendicular to the oral-aboral axis of the body column. Grafting experiments were performed using adult tissues only from a clonal colony, following the cutting protocol described above and carried as follows: 1) Head and physa were surgically removed from relaxed animals; 2) The body column was isolated and opened along the oral-aboral axis of the polyp with microsurgical scissors (Fine Science Tools GMBH #15100-09, Heidelberg, Germany); 3) If required, the mesenteries were gently removed mechanically from the epithelia using forceps (Rubis Grip Tweezers, style 3C) and microsurgical scissors 4) Isolated epithelia from the body wall were forced to contact

the freshly isolated mesenteries approximately 5 to 10 min after tissue isolation and the graft was maintained with a human hair allowing the wounds to heal properly; 5) After three days the hair was removed to avoid any mechanical constraints or tissue damages during the regenerating period. Isolated fragments and grafts were transferred into a new dish (or rinsed at least five times to remove $MgCl_2$) and maintained in 1/3 ASW at 22°C (if not stated otherwise) for the duration of the experiments.

Fixation, DNA, actin labeling

After relaxing adult or juvenile polyps as well as isolated body parts in $MgCl_2$ for 10-15 minutes, animals were fixed in 4% paraformaldehyde (Electron Microscopy Sciences # 15714) in 1/3 ASW during 1 hour at 22°C or overnight at 4°C. Fixed animals were washed three times in PBT 0.2% (PBS1x + Triton 0.2%). To analyze the general morphology, Hoechst staining (Invitrogen #33342, Carlsbad, CA, USA) at 1/5000 was used to label the DNA/nucleus and BODIPY® FL PhallAcidin 488 (Molecular Probes #B607, Eugene, OR, USA) staining at 1/200 to label actin microfilament (cell membranes and muscle fibers).

Cell proliferation and "pulse and chase" experiment

To detect cellular proliferation Click-it EdU (5-ethynyl-2'-deoxyuridine) kits (Invitrogen # C10337 or # C10339, Carlsbad, CA, USA) were used following the protocol from [59]. To visualize cell proliferation at a given time point EdU incubation was carried out during 30min. For the "pulse and chase" experiment EdU incubation was performed during 1h, then washed 5 times and chased for the period of interest. In order to identify

of the Label Retaining Cells (LRCs), animals were incubated for one week with EdU, then chased up to 11 weeks for juveniles or 3 to 5 month for adults.

Irradiation

For irradiations experiments, animals where placed in a 10cm diameter petri dish with 15ml 1/3 ASW. Irradiations at 100 and 300 Grays where performed on the juvenile polyps using a X-ray irradiator (CP-160 Cabinet X-Radiator, Faixitron). After irradiation, animals were recovering during 4 hours in their culture medium (1/3ASW) at room temperature before further cutting experiments.

Imaging

Live animals were imaged using a protocol described in [63]. The imaging setup was composed of either with a Zeiss Stereo Discovery V8 Discovery or a Zeiss Axio Imager A2 (both Carl Zeiss Microscopy GmbH, Jena, Germany) equipped with a Canon 6D (Canon) or a Axiocam 506 color camera (Zeiss) digital camera, triggering two external Canon Speedlite 430 EX II Flashes and controlled by the Canon Digital Photo Professional software (Canon Inc, Tokyo, Japan). Images were edited using Adobe Lightroom 5 and/or Photoshop CS6 software (Adobe Systems Inc, San Jose, CA, USA). Labeled animals were analyzed using a Zeiss LSM Exciter confocal microscope running the ZEN 2009 software (Carl Zeiss Microscopy GmbH, Jena, Germany) from the IRCAN imaging platform (PICMI). Each final image was reconstituted from a stack of confocal images using Z-projection (maximun intensity or standard deviation) of the ImageJ

217 software (Rasband, W.S., ImageJ, U. S. National Institutes of Health, Bethesda,

218 Maryland, USA, http://imagej.nih.gov/ij/, 1997-2014).

219

Results

The regenerative capacity of the physa is age dependent

In order to assess if all body parts of *Nematostella* possess similar regenerative capacities and if those limits are age dependent, we dissected adult and juvenile *Nematostella* into several isolated body parts. Following dissection, we analyzed each parts capacity to regenerate the missing oral or aboral structures within seven days (Figures 1, Additional file 1: Figure S1). Throughout the manuscript the isolated body parts that are tracked to score regeneration are indicated as follow: [name of the isolated part]. As an example, when a tentacle is isolated and tracked for it is ability to regenerate, it is indicated as [tentacle]. [full body column + physa] is the equivalent of the sub-pharyngeal amputation experiment performed in previous studies [59,62] (Figures 1Ac,c', Bh,h', C) and is considered as positive control in the corresponding experiments.

We first addressed the capacity of isolated body parts to regenerate missing oral structures (oral regeneration) and we observed that most body regions isolated from either juvenile or adult polyps regenerate within 144hpa. The only exception was the isolated juvenile (but not adult) physa that failed to regenerate missing oral features (pharynx, mouth, tentacles, Figure 1Aa-e, a'-e', Bf-j, f'-j', C). The capacity of body parts to regenerate is correlated with the presence of massive cell proliferation at the amputation site throughout regeneration (Figure 2A, B). Massive cell proliferation was also observed at the amputation site (Figure 3Aa,b) and is required for regeneration of the adult [physa] (Figure 3Ac,d). Interestingly, no or very little cell division was detected in juvenile [physa] (Figure 3Ba,b). These observations show that for the various isolated

243 body parts the capacity to regenerate is associated to cell proliferation, suggesting similar
244 cellular mechanisms involved in this process along the different regions of the polyp.
245 They also highlight that existing age-dependent differences in the regenerative capacity
246 of *Nematostella* are body part specific.
247
248 A similar conclusion was obtained when analyzing the regenerative capacity of
249 isolated juvenile or adult oral body regions to reform aboral structures (aboral
250 regeneration) (Additional file 2: Figure S2). Only juvenile [tentacles + full pharynx + half
251 body column] and [body column], as well as adult [tentacles + full pharynx], [tentacles +
252 full pharynx + half body column] and [pharynx] regenerated (Additional file 1: Figure
253 *S2Ad, d', Bg-j, g'-j', C*). Intriguingly though, we did not observed massive cell
254 proliferation at the amputation site, neither for the regenerating nor the non-regenerating
255 isolated body parts (Additional file 3: Figure S3), suggesting different cellular strategies
256 involved in the oral *vs* aboral regeneration processes.
257
258 Taken together these experiments clearly illustrate the existence of limits in the
259 regenerative abilities of distinct *Nematostella* body parts (i.e. the tentacles) that is also
260 varying in an age-dependent manner (i.e. physa). While aboral regeneration seems to
261 involve mainly cell/tissue rearrangements, importantly, the capacity of body parts to
262 reform missing oral structures is tightly linked to the ability of cells to re-enter mitosis,
263 suggesting qualitative variations in the tissues that form the body of *Nematostella*.
264
265 *Mesenteries are present in the adult but not in the juvenile physa*

Intrigued by the observation that some body parts were able to perform oral regeneration when isolated from adults but not from juveniles (e.g. physa, Figure 1Aa,a', Bf,f', C), we analyzed in detail the anatomy of the physa in juvenile *vs* adult polyps (Figure 4). DIC microscopy revealed that in addition to the size variation between juvenile and adult physa, a major difference exists in the thickness and elongation of the longitudinal muscle fiber extensions within the mesenteries (Figure 4a,c). While in adult physa we observed opaque longitudinal extensions from the aboral end of the mesenteries towards the aboral-most tips of the physa (Figure 4c), in juvenile physa, we couldn't detect those longitudinal extensions (Figure 4a). We further performed confocal imaging of the juvenile and adult [physa] using phalloidin to label actin microfilaments (longitudinal and transversal muscle fibers as well as cell cortex) and DAPI to label the nucleus (Figure 4b,b',d,d'). We observed that in adult [physa], the longitudinal muscle fibers are considerably thicker compared to the ones present in juvenile tissues (Figure 4b,d). Orthogonal projection of these confocal images further revealed significant differences in the organization of the longitudinal muscle fibers in juvenile or adult [physa] epithelia (Figure 4b',d'). In juvenile [physa], we observed a discrete protrusion from the longitudinal muscle fibers toward the gastric cavity (Figure 4b'). In contrast, the longitudinal muscle fibers of the adult [physa] are thick and shaped in a characteristic manner (Figure 4d'). Within the adult endoderm, they form a stalk at the base of the epithelium that becomes undulated more distally (Figure 4d'). Interestingly, this particular form is strikingly similar to the organization of parietal muscles that support the developing mesenteries [36]. Thus, these observations show the presence of forming

288 mesenteries only in the adult physa and suggest a correlation between the presence of the
289 mesenteries and the capacity of a given tissue to regenerate.
290
291 *Mesenterial tissue is required for cell proliferation and regeneration*
292 While in the juvenile [physa] no or very little mitotic activity was detected in the majority
293 of cases (Figure 3Ba, a'), 24 out of 63 juvenile [physa] displayed localized cell
294 proliferation at the amputation site (Figure 3Bb-c,b'-d'). Interestingly, DIC and
295 fluorescence imaging revealed that the observed localization and intensity of cellular
296 proliferation were linked to the presence and the amount of remaining mesenterial tissues
297 in the juvenile [physa] (Figure 3Ba'-d'). This observation strongly supports the idea that
298 the presence and amount of mesenteries remaining in the isolated body part, are
299 associated to cell proliferation during regeneration.
300
301 In order to directly test our hypothesis that mesenteries are crucial for cell
302 proliferation and regeneration in *Nematostella*, we performed further tissue isolation
303 experiments in adults. By cutting twice transversally, we isolated a part of the mid-trunk
304 region that we named [BE + mes] (Body wall Epithelia *plus* mesenteries). We then
305 opened it longitudinally to separate the body wall epithelia [BE] from the mesenteries
306 [mes], and cultured the [BE] and [mes] separately (Figure 5, Additional file 4: Figure S4).
307 We then analyzed daily if the isolated tissues [BE] or [mes] or the combination of both,
308 [BE + mes], are able to regenerate a fully functional polyp. The [mes] did not regenerate
309 (90 out of 90 cases) but instead, began to fragment one day after isolation, and
310 progressively degraded over time (Figure 5a-c). Surprisingly, while the wound healed,

311 none of the [BE] regenerated neither and they remained intact even after 25 days post
312 isolation (33 out of 34) (Figure 5d-f). Only the [BE + mes] regenerated 10 days after
313 tissue isolation (27 out of 39, Figure 5g-i) and the resulting polyps were able to feed
314 (Additional file 5: Figure S5). To further analyze the importance of the mesenteries to
315 induce regeneration in the surrounding [BE], we performed rescue experiments by
316 grafting [mes] to the endodermal component of the [BE]. Interestingly, nearly half of the
317 grafts regenerated a polyp (6 out of 14 cases, Figure 5j-l). However, regeneration was not
318 complete and none of the regenerated polyps were able to feed. After several weeks, one
319 of them lost its tentacles and all reduced in size (data not shown).
320
321 To advance our understanding of the role of the mesenteries in inducing
322 regeneration, we analyzed cell proliferation at 24, 72 and 168hpa (7dpa) in the isolated
323 tissues described above. While at 24hpa, we did not observe cell proliferation neither in
324 [BE] nor in [BE + mes], at 72 and 168hpa we detected massive and localized cell
325 proliferation only in the [BE + mes] (Figure 6a-f). At those time points, cell proliferation
326 was detected in a density gradient of EdU+ cells in the tissue, allowing us to determine
327 the site where the future tentacles will form (Figure 6e-f). Taken together, our data
328 clearly show that i) the presence of [BE] is required to maintain the integrity of the
329 mesenteries, and that importantly, ii) the mesenteries are required and possess the
330 capacity to induce cell proliferation as well as regeneration of the body wall epithelia.
331 Thus, a crosstalk between [mes] and [BE] is required for the regeneration process in
332 *Nematostella,* with a particularly crucial role of the mesenteries in the induction of this
333 phenomenon.

334 *Label retaining cells are present in* Nematostella *tissues*

335 In whole body regeneration models, tissues lacking regenerative capacities have
336 been associated to the absence of undifferentiated stem cells in this compartment (e.g.
337 planarian pharynx [9-11], *Hydra* tentacles [12,13]). In the previous set of experiments we
338 have identified the juvenile physa that, in contrast to its adult counterpart is devoid of
339 mesenteries, as a body part lacking regenerative capacity. Thus an appealing hypothesis
340 is that the mesenteries are one compartment that acts a as a potential source of adult stem
341 cells involved in regeneration in *Nematostella*.

342

343 Quiescence or slow cycling is among the characteristics of vertebrate adult stem
344 cells that participates in the protection of their genomic integrity [64]. In order to identify
345 the existence of slow cycling / quiescent cells populations in *Nematostella*, we carried out
346 label retaining experiments used in many vertebrate models to identify tissue specific
347 stem cell populations [65-69]. After a one-week EdU pulse and extensive rinsing steps in
348 uncut juveniles and adults, the labeled animals were feed once (juveniles) or twice
349 (adults) per week during the 11 weeks (juveniles) or 39 days (adults) periods of the chase
350 (Figure 7).

351

352 Starting at seven weeks or 39 days after the EdU pulse in juveniles or adults
353 respectively, we began to distinguish isolated and randomly localized EdU+ label
354 retaining cells (LRCs, Figure 7). Those LRCs were detected as expected in the
355 mesenteries of juvenile and adult polyps (Figure 7C,D). Note that in addition to randomly
356 dispersed LRCs in adult mesenteries, we also observed dense EdU+ cells in a restricted

region close to the gametes, suggesting the presence of germ line precursors in this specific location (Figure 7D, Additional file 6: Figure S6g,g').

To our surprise we also detected LRCs within the body wall epithelia (Figure 7A,B. Interestingly, we detected LRC pairs in juveniles and adult epithelia, suggesting that a subpopulation of quiescent cells are able to divide to maintain tissue homeostasis in *Nematostella* (Figure 7Ae,e',f,f',Bh,h'). In adults, the density of LCRs after 39 weeks seemed reduced in the endoderm compared to the ectoderm, suggesting that the cellular renewal takes place faster in the endoderm than in the ectodermal (Additional file 7: Figure S7a,a',b,b'). To reinforce the idea that we have detected quiescent/slow cycling cells in *Nematostella*, LRCs were still detected in the epithelia of the body wall (as well as in the mesenteries) five months after the initial EdU pulse (Additional file 8: Figure S8k,k'). However, while after 39 days of chase LRCs were still detected in the tentacles, after 5 months no more LRCs were observed in this part of the body (Additional file 8: Figure S8h-j,h'-j'), suggesting that the cellular turnover (causing the elimination of the LRCs) in the tentacle region is increased compared to the body column.

To make sure that the LRCs we detected are not all terminally differentiated cells, we analyzed the nuclear morphology and organization of those EdU+ cells. While we detected differentiated cells such as cnidocytes, excretory cells and batteries of nematocysts (Additional file 7: Figure S7d-f,d'-f'), we also observed a subpopulation of cells with highly condensed DNA (Additional file 7: Figure S7c,c'), reminiscent of stem cell nuclei in *Hydractinia* [22]. The presence of LRCs in the mesenteries (other than

potential germ line precursors) as well as in the epithelia that are able to re-enter the mitotic cycle under physiological conditions, further support the presence of adult stem cells in the anthozoan *Nematostella*.

Irradiation resistant LRCs in the mesenteries and response to the amputation stress

The capacity to retain EdU labelling is one feature of slow cycling/quiescent stem cell populations that thus represent an increased resistance to irradiation. Another characteristic is the ability to re-enter the cell cycle after a challenge (e.g. amputation stress) [64]. In order to test this ability in *Nematostella*, we inhibited mitosis in uncut animals using X-ray irradiation. As expected, no more cell proliferation was detected four hours after irradiating the animals at 100Gy (Additional file 9: Figure S9a,a',b,b'). In order to analyze if mitotic activity can re-emerge in the irradiated animals, we performed EdU incorporation at various time points following irradiation on uncut polyps (Additional file 9: Figure S9c-e,c'-e'). Interestingly, we observed EdU+ cells starting at 96hours post irradiation (hpirr) that were dispersed randomly within the mesenteries and the basal part of the pharynx but not at all in the epithelia (Additional file 9: Figure S9e,e'). These data clearly show that a pool of cells within the mesenteries and the basal part of the pharynx is able to escape the effects of irradiation.

In order to test if this small pool of irradiation resistant quiescent/slow cycling cells is sufficient to allow proper regeneration, we performed a sub-pharyngeal amputation four hours after irradiation. Doing so, we observed that regeneration was impaired. More precisely, the majority of irradiated animals were blocked prior to the formation of the

403 pharynx at step 2 of the sub-pharyngeal oral *Nematostella* regeneration staging system
404 [62] (100Gy: Figure 8A, Additional file 10: Figure S10i,i'; 300Gy: Additional file 11:
405 Figure S11b,b', Additional file 12: Figure S12). To analyze the capacity of the
406 quiescent/slow cycling cells to respond to the amputation stress, we repeated the same
407 experiment (sub-pharyngeal amputation of irradiated polyps) that was followed by EdU
408 labeling at various time points post dissection. To our surprise, we detected the presence
409 of EdU+ cells in the most oral part of the mesenteries already at 48hpa in the amputated
410 polyps (Figure 8Be,e'). Later (120hpa), in addition to the ones in the oral tips of the
411 mesenteries, we also observed EdU+ cells in the epithelia at the amputation site (100Gy:
412 Additional file 10: Figure S10i,i'; 300Gy: Additional file 11: Figure S11b,b'). While
413 quiescent/slow cycling cells that escape irradiation are able to re-enter the cell cycle in
414 uncut as well as cut polyps, their timing of emergence and dispersion is different. They
415 are either detected 96hpa and distributed along the oral-aboral axis of the mesenteries in
416 uncut animals, or restricted to the oral most part of the mesenteries in dissected polyps
417 starting 48hpa. Latter observation suggest that quiescent/slow cycling cells are migrating
418 from the aboral region of the mesenteries towards the oral most part of those structures in
419 response to the amputation stress.
420
421 Taken together these results show that i) the quiescent/slow cycling cells of the
422 mesenteries alone are not sufficient to allow full regeneration, ii) that at least an
423 additional pool of fast cycling cells (the ones affected by irradiation) are required for
424 reformation of lost body parts and iii) that the LRCs of the mesenteries that escape the
425 effects of irradiation, are activated by the amputation stress by displaying mitotic activity

and by migrating towards the amputation site. Thus, we now provide a series of evidences that highlight the presence of quiescent/slow cycling stem cells in *Nematostella*, in particular, those located within the mesenteries.

LRCs are migrating from the mesenteries to the body wall epithelia

We have shown that a crosstalk between the mesenteries and the epithelia is required for cell proliferation/regeneration and that quiescent/slow cycling stem cells are potentially migrating from the mesenteries to the surrounding epithelia in response to the amputation stress. To test this hypothesis, we designed a protocol that combined EdU pulse and chase with grafting experiment. More precisely, we labeled LRCs of the entire polyp and isolated its mesenteries, named [mesLRC] (LRC stained mesenteries). We then grafted the [mesLRC] to the endodermal component of the [BE] from an unlabeled animal (Figure 9A). After 14 days, 3 out of 18 grafts regenerated. Nonetheless, all 18 grafts were fixed in order to chase the EdU staining and determine the localization of LRCs in the chimeric animals. To our surprise, we not only observed LRCs in the previously unlabeled [BE] (5 out of 18 cases), but also far from the [mesLRC] source (Figure 9Ba). In one of the regenerated [mesLRC] [BE] grafts, a large amount of LRCs have even migrated towards the newly formed tentacles (Figure 9Bd). This clearly demonstrates that LRCs are able to migrate from the mesenteries towards the epithelia, and even within the epithelia to integrate specific regions. Importantly, we also observed LRC pairs (in addition to single LRCs), showing that the LRCs that migrated from the [mesLRC] to the [BE] were able to divide and are not post-mitotic (Figure 9Bb,c). A detailed analysis of the DNA of migrating LRCs using confocal microscopy revealed that

i) their nucleus is round, ii) very similar in size, iii) posses a compact DNA and iv) the majority is located in the endoderm of the [BE] (Figure 9C). Latter observation strongly suggests that the graft re-establishes the physical contact between the endodermal components of the mesenteries and the [BE]. In sum, we now have clear evidence that LRCs, or their immediate progeny, are able to migrate from the mesenteries towards the body wall and tentacle epithelia under stress conditions where they may participate in regenerating missing body parts.

LRCs localized in the epithelia respond to the amputation stress

In addition to the clearly defined pool of mesenterial LRCs, we have also observed LRCs within the epithelia that were however, less numerous compared to the mesenterial ones (Figure 7). To perform a detailed characterization of all LRCs present in *Nematostella*, we also analyzed the dynamics of LRCs localized in the epithelia of the body wall during regeneration. We performed sub-pharyngeal amputation on LRCs positive adult polyps (Figure 10A) and analyzed at various regeneration time points (24-192hpa) i) the localization of the LRCs, ii) their ability to divide and form clusters in response to the amputation stress and iii) their becoming in the newly regenerated head (Figure 10B). The LRCs of the mid-body and aboral regions remained largely unaffected. However, we detected a general, although variable, accumulation of LRCs as well as the presence of LRC clusters at the amputation site starting at 24hpa (Figure 10Ba-d,a'-d'). This variability could be either associated i) to the different metabolic states of each individual or ii) to the increased division rate at the amputation site at later stages that may cause the dilution of the EdU signal or iii) both. Importantly though, we detected

472 single LRCs as well as pairs of LRCs in the newly formed tentacles 8 days post-
473 amputation (192hpa) (Figure 10Be-e'').
474
475 Taken together, our data show that the LRCs of the epithelia, although they are
476 not able to escape the effects of irradiation, i) are activated in response to the amputation
477 stress by dividing and accumulating at the amputation site and ii) participate in the newly
478 formed head (e.g. tentacles epithelia), providing clear evidence that those epithelial LRCs
479 are actively involved in tissue renewal and thus, also possess stem cell-like characteristics.
480
481 *Accumulation of fast cycling cell at the amputation site during oral regeneration*
482 We have seen that the mesenterial LRCs (reactivated during regeneration
483 following irradiation) alone are not sufficient to promote full regeneration. This shows
484 the necessity of a tissue crosstalk and in particular, the requirement of another pool of
485 (stem) cells localized in the body wall epithelia. During the irradiation experiment, we
486 blocked cell proliferation in cells that are undergoing mitosis including fast cycling cells
487 required for tissue homeostasis. In order to test if a population of fast dividing cells from
488 the uncut animal also migrates to the wound site during regeneration, we performed a 1h
489 EdU pulse in uncut animals followed by extensive washes to eliminate any excessive
490 EdU. This EdU pulse labels the fast dividing cells involved in tissue homeostasis (Figure
491 11Aa). We then performed a sub-pharyngeal amputation and chased the EdU+ cells
492 during the process of regeneration from 0 to 120hpa (Figure 11A,B).
493

494 In uncut control animals, EdU+ cells were randomly dispersed throughout the
495 body wall epithelia as well as in the mesenteries for all analyzed time points [59](Figure
496 11Aa-d, Additional file 13: Figure S13). Starting at 24 hours post-pulse, first homeostatic
497 EdU+ cell divisions are detected (still in a dispersed manner) in uncut animals, as
498 indicated by the presence of EdU+ cell pairs (Figure 11Ab-d). Interestingly, in sub-
499 pharyngeally amputated polyps, we observed a strong accumulation of EdU+ cells in the
500 oral regions of the mesenteries while their remaining aboral parts progressively become
501 devoid of those cells (Figure 11B). This accumulation, indicating amputation-site-
502 directed cellular migration within the mesenteries is already visible at 24hpa Figure
503 11Bi,j, while EdU+ cells are still randomly located within the epithelia (Figure 11Ae,f).
504 However, starting at 48hpa, EdU+ cells accumulate massively in a restricted region of the
505 epithelia at the amputation site and, in a few cases (48hpa: 9 out of 31), a zone depleted
506 of EdU+ cells is observed in the region below the massive accumulation of EdU+ cells
507 (Figure 11Ag,h).
508
509 Those observations are further quantitatively supported by carefully counting individual
510 Edu + cells in three different zones (Z1', Z1'' and Z2) of the body epithelia along the
511 oral-aboral axis of the uncut *vs* cut animal during regeneration (Additional file 14: Figure
512 S14). In addition to the difference in the average number of EdU+ cells in zone Z1' in
513 uncut (sub-pharyngeal region) *vs* cut (amputation site), this cell counting revealed clear
514 differences in the Z1" (lower mid-body region) and Z2 (aboral end) zones for the same
515 conditions. In fact, while the average number of EdU+ cells in Z1" and Z2 is constant or
516 decreasing respectively in regenerating animals, it is increasing in both zones in uncut

517 controls (Additional file 14: Figure S14). In sum, these results show that fast cycling cells
518 (required for regeneration as eliminated during irradiation) from the region below zone
519 Z1' of the body wall epithelia, migrate towards the amputation site and in cooperation
520 with LRCs, actively participate in the renewal of missing tissues.
521
522
523
524
525
526
527
528
529
530
531
532
533

Discussion

In the present study, we have highlighted the unexpected role of the mesenteries not only as a reservoir of quiescent/slow cycling stem cells, but also as the tissue harboring the signal to induce cell proliferation and regeneration in *Nematostella*. Long-term EdU pulse and chase experiments revealed the presence of quiescent/slow cycling cells (LRCs) that respond to the amputation stress by reentering the mitotic cycle, accumulation at the wound-site and participate in the reformation of missing structures. Combining classical graft experiments with EdU pulse and chase experiments, revealed cellular migration from the mesenteries to the epithelia, as well as toward the amputation site in response to the amputation stress. We further showed that LRCs alone are not sufficient and that homeostatically fast cycling cells are required for regeneration. In sum, our present work has not only revealed the requirement of a tissue crosstalk between the mesenteries and the epithelia of the body wall to initiate the cellular dynamics underlying regeneration but importantly also the synergic effect of fast cycling cells and slow/quiescent stem cells to enable full reformation of lost body parts. This study provides also for the first time in an anthozoan cnidarian a set of strong evidences for the presence of adult stem cell populations that are directly involved in the regenerative response.

We thus propose a mechanistic model for head regeneration in *Nematostella,* in which the mesenteries, once in contact with the epithelia of the amputation site (Step 1, [62]) emit a regeneration-initiating signal that activates fast and slow-cycling stem cell populations from the mesenteries as well as the epithelia by inducing their division and

557 migration toward the wound site. Importantly, a synergic effect between those two stem
558 cell populations is required to pursue and complete the regeneration process. The
559 regeneration inducing signal emitted by the mesenteries, the mechanism of synergic
560 cooperation between the two stem cell populations and whether de- or trans-
561 differentiation processes are also involved in the tissue repair and regeneration program
562 of *Nematostella*, remains to be investigated.
563
564 *Distinct cellular mechanisms between oral* vs *aboral regeneration in Cnidaria*
565 By comparing the regenerative capacity of various body parts to reform missing
566 oral as well as aboral structures, we observed that regeneration of aboral tissues does not
567 involve massive cellular proliferation at the amputation site, while oral regeneration does.
568 These data suggest that aboral regeneration either i) uses a different cellular mechanism
569 than the one described for oral regeneration in order to reform the missing physa and/or
570 ii) that the requirement of regenerating aboral tissues is less urgent (and thus does not
571 require massive localized cell proliferation) than quickly reforming a missing head region
572 that is more complex and crucial for feeding and defense. A distinct cellular mechanisms
573 for oral *vs* aboral regeneration has been recently described in the cnidarian hydrozoan
574 *Hydra* and *Hydractinia* [20,22] supporting the idea that using different mechanism to
575 regenerate opposite part of the body in a same system seems to be a conserved feature
576 among Cnidaria. The studies performed in Hydrozoa show that similar to our
577 observations, no massive cell proliferation is detected at the aboral amputation site
578 [20,22]. In *Nematostella*, while we also observe a slight reduction in tentacle size during
579 aboral regeneration that could contribute to the reformation of the physa via tissue

580 reorganization, we have no evidence for a complete transformation of the body column
581 into an aboral fate prior to re-growing a fully functional polyp. However, recent work on
582 *Nematostella* shows a clear difference in the transcriptional response of the oral *versus*
583 aboral regeneration process [61]. This study also shows that the early molecular response
584 (8hpa) to the amputation stress is more similar between oral *vs* aboral regions, compared
585 to later time points (24 and 72hpa) [61]. Interestingly, our previous study on *Nematostella*
586 regeneration revealed that early oral regeneration steps (from step 0 to step 1; between 0
587 to 24hpa) are cell proliferation independent, while the later ones (from step 2 to step 4,
588 between 24 to 120hpa) are cell proliferation dependent [62]. Thus, in *Nematostella*, the
589 mechanisms driving the early steps of tissue regeneration such as wound healing seem
590 similar between oral *versus* aboral regeneration as they are both cell proliferation
591 independent. However, additional experiments are required to gain a better understanding
592 of the cellular and molecular mechanisms involved in aboral regeneration in
593 *Nematostalla,* in particular during later regeneration phases, when initial wound healing
594 and early response is completed.
595
596 *Regenerative capacity of a given body part is age-dependent*
597 It has been previously shown that oral regeneration after sub-pharyngeal
598 amputation in *Nematostella,* occurs at a comparable time-scale in both juveniles and
599 adults and that cellular proliferation is required in both cases [62]. Our present study
600 revealed that clear variation in the capacity to regenerate exists in one given body part
601 depending on the age of the organism. The obtained data show that the tissue composition
602 within a given body region is changing with age. In particular, the isolated physa

603 regenerates only in adults, but not in juveniles that are unable to induce sufficient cellular
604 proliferation, probably by the lack of i) stem cell population(s), ii) initiation signal(s) or
605 both. In addition, this approach was useful to identify which body part/structure of
606 *Nematostella* is required for the initiation of regeneration and to orient our research on
607 the potential stem cell population(s) involved in the regeneration process.
608
609 *Mesenteries are required and sufficient to induce cell proliferation and regeneration*
610 Taking advantage of the differential regenerative capacity of juvenile and adult
611 physa, we identified the mesenteries as crucial structures to induce cellular proliferation
612 and subsequent regeneration in the surrounding tissues. By performing tissue dissociation
613 and grafting experiments, we have shown that isolated mesenteries, grafted back to the
614 remaining [BE] of the same individual, are sufficient to induce regeneration. Extending
615 this finding to other body parts of juveniles that did not regenerate when isolated such as
616 [tentacles], [tentacles + half pharynx], [tentacles + full pharynx] and [pharynx], it seems
617 plausible that the common factor explaining the lack of regeneration in those juvenile
618 body parts are the missing or not completely formed mesenteries. [tentacles] or [tentacles
619 + half pharynx] isolated from adults did not regenerate neither, while [tentacles + full
620 pharynx] or [pharynx] did. Tentacles clearly lack mesenterial tissues and interestingly,
621 the mesenteries are anchored to the pharynx in its aboral regions. As the half pharynx that
622 remained with the tentacles in [tentacles + half pharynx] corresponds to the oral half of
623 the pharynx, the absence of regenerative capacity in juvenile and adult [tentacles] or
624 [tentacles + half pharynx] can thus be linked to the absence of mesenteries in those body
625 parts. Fully formed mesentery anchors are present in the adult pharynx that are sufficient

626 to induce regeneration from [tentacles + full pharynx] or [pharynx]. In analogy to our
627 findings in the juvenile physa, we expect that the mesenterial anchors, or at least
628 important components of it (i.e. stem cells), in the juvenile pharynx are not fully formed
629 or are absent. This may explain the absence of regenerative capacity of those isolated
630 body parts.
631
632 One puzzling observation in the graft experiments (restoring the regenerative
633 capacity) was that the regenerated animals possessed a tentacle crown but not a mouth
634 and were therefore unable to feed. One probable explanation for this is the number of
635 mesenteries required for full regeneration. In the graft experiment performed in our
636 present study only one mesentery has been grafted into the epithelia leading to a partial
637 regeneration (head without mouth/pharynx). By testing the removal of only 7, 6 or 5
638 mesenteries on 8 total from the adult body wall epithelia, we have observed that at least
639 two mesenteries are required for proper mouth formation. In none of the cases in which
640 only one mesentery was left in contact with the body wall epithelia, the regenerated
641 polyps were able to fed, showing that only partial regeneration occurs (data not shown).
642 This evidence for the requirement of at least two mesenteries for proper pharynx
643 reformation is further enhanced by previous observations that during oral regeneration the
644 two mesenteries fuse to one to each other, and that the fused oral parts of the mesenteries
645 give rise to the vast majority of the newly formed pharynx [62].
646
647 *A tissue crosstalk is required for initiating a regenerative response*

The observation that the mesenteries are required to induce regeneration in the surrounding epithelia leads to three main hypotheses concerning the mechanism involved: 1) A long-range diffusing "regeneration" signal emitted by injured mesenteries is required to initiate cellular proliferation in the surrounding epithelia. 2) The physical integrity of the tissue that links the mesenteries to the body epithelia is important to relay the "regeneration" signal. 3) A pool of stem cells (or their offspring) migrates from the mesenteries to the body wall epithelia to initiate the regeneration process. We tested the first hypothesis by incubating the isolated body wall epithelia in close but not physical contact with isolated pieces of mesenteries in the same wells. In none of the cases the body wall epithelia regenerated (data not shown), suggesting that the molecular induction signal (if there is any) from the mesenteries is not sufficient alone, or that it is too diluted in the well, to induce regeneration of the epithelia. Alternatively, it might also be possible that only endodermal cells respond to the induction signal to transform it into a regenerative response. In this case, the fact that the isolated epithelia wounded and closed with the endodermal cells inside prevents the signal to target the responsive cells. While additional experiments are required to fully address hypothesis 1, we currently favor hypothesis 2 and 3 to explain the role of the mesenteries in the regeneration process of *Nematostella*.

The importance of physical tissue crosstalk during regeneration has been studied during vertebrate intestinal epithelium regeneration in which the connective tissues have been shown to be crucial for the regeneration of the epithelium [70]. In addition, cell/cell contact molecules such as integrins are known to be involved in the regeneration process

in vertebrates [71,72] [73]. The migration of stem cells to the amputation site has been shown for regeneration of complex structure [74,75] and it has been proposed that mechanical stress induces cell migration as in smooth muscles [76]. Our study has provided clear evidences for a cellular transfer of cells from the mesenteries to the epithelia as well as the existence of two populations of cells that have stem cells characteristics (Hypothesis 3). The observation that the mesenteries disintegrate when isolated from the body wall epithelia highlight the importance of a tight and physical tissue interaction between the epithelia and the mesenteries to maintain the integrity and/or homeostasis of the mesenteries (Hypothesis 2). Hypothesis 2 and 3 are further reinforced by the fact that the process of regeneration is delayed in graft experiments compared to [BE + mes] (14 *vs* 10 days, respectively). This could be explained by the fact that the tissue connecting the mesentery and the body wall epithelia [62] needs to be first reformed, before either the inductive signal can be relayed, or before the stem cell population can migrate from the mesenteries to the body wall epithelia.

Migration of different pools of cells during regeneration

Our work highlights evidences that cell migration occurs during *Nematostella* regeneration as it is the case in others invertebrate and vertebrate regeneration models studied so far [1]. These evidence are: i) LRCs migrate from the mesenteries to the surrounding epithelia, ii) fast cycling cells involved in tissue homeostasis migrate to the amputation site, and iii) following irradiation, slow cycling EdU+ cells within the mesenteries that escape irradiation accumulate the most oral part of the mesenteries, while EdU+ cells are randomly dispersed in the mesenteries in irradiated uncut animals.

These data show that this population of cells re-entering the cell cycle in irradiated animals migrate to the amputation side during regeneration. However, latter cell population is not sufficient alone to fully complete regeneration as the regeneration process in irradiated polyps is blocked at step 2 of the sub-pharyngeal *Nematostella* staging system [62]. We recently showed that inhibition of cell proliferation using Hydroxy Urea during *Nematostella* regeneration, blocked the regeneration process at step 1 [62], suggesting that the slow cycling, irradiation-resistant cells that re-entered the mitotic cycle in response to the amputation stress are crucial to transition at least from step 1 to step 2.

In *Nematostella*, although we were able to detect a "first wave" of migrating cells only between 24-48hpa, we cannot exclude that cell migration of other cell populations also occurs at earlier time points between 0 to 24hpa, as it has been shown in *Hydra* [20]. The potential second "wave" of cell migration, reflected by the decrease in the number of the EdU+ cells in zone Z2 (most aboral part of the animal) during regeneration, might correspond to a replacement of stem cells populations in a zone that got depleted of it. This kind of stem cell replenishment has been shown during tissue homeostasis or tissue transplantation experiments in *Hydra* to repopulate a tissue that was i-cell deficient [77] [78]. Our experiments show that fast as well as slow cycling cells are able to migrate during *Nematostella* regeneration, however, we currently don't know if the migrating cells are the stem cells or their progeny. Further characterization of the molecular identity of those migrating cells as well as the development of *in vivo* tools is required in *Nematostella* to answer this question.

Stem cells in Anthozoa

Prior to the present study, cells populations with clear stem cell characteristics have not been described in *Nematostella* or more generally in anthozoan cnidarians (sea anemones, corals) [32,57,59]. Our present work highlights the existence of two populations of proliferating cells that are synergistically required for regeneration: i) one pool, composed of slow cycling/quiescent cells (LRCs) and ii) another pool, composed of fast cycling cells involved in tissue homeostasis in the uncut animal. Both cell populations possess features that are characteristic for stem cells: 1) The behaviour of the slow cycling/quiescent/label retaining cells (LRCs) *per se*, as it is one important feature of adult stem cells that is deployed in mammalian stem cells to preserve genomic integrity [64,69]. These slow cycling/quiescent cells are able to escape X-ray irradiations and respond to the amputation stress by migrating and accumulating towards the wound site, where they actively divide and participate in the reformation of lost structures. While the potency of those LRCs has not been properly addressed yet, we already observed that they are able to give rise to sensory cells within the regenerated tentacles. 2) The fast cycling cells, respond to the amputation stress by migrating towards the amputation site where they actively divide and are required for regeneration, probably for later regeneration steps (3 and 4). In the hydrozoans *Hydra* and *Hydractinia*, fast cycling stem-cells (i-cells and/or their progeny) also divide and migrate to the amputation site and actively participate in the regeneration process [20,22]. Thus, our results suggest a conserved pool of fast cycling stem cells in cnidarians that are involved in tissue homeostasis and regeneration.

740

741 Stem cell/pluripotency markers in ctenophores and cnidarians are known to
742 include the germ lines markers *piwi*, *vasa*, *nanos* and *PL10* [22,79-84] [85]. A previous
743 study in *Nematostella* analyzed the expression pattern of those genes (with the exception
744 of *piwi*) from early development to the primary polyp stage [86]. In the juvenile, *Nvnos1*
745 is found in some patches of cells in the ectodermal epithelia of the body wall. The authors
746 suggested that these patches of *Nvnos1*+ cells are "population of nematocyst precursors
747 with stem cells characteristics" [86]. However, all other analyzed germline genes *NvPl10*,
748 *Nvvasa1*, *Nvvasa2* and *Nvnanos2* are expressed solely in the mesenterial tissues, excluded
749 from the epithelia of the body wall and interestingly, are not detected within the physa of
750 juveniles [86]. Those data combined with our current work further strengthen the idea
751 that a specific stem cell population, able to respond to the amputation stress is located in
752 the mesenteries of *Nematostella*.

753

754 However, it is important to note that the germ line of anthozoans is located in the
755 mesenteries [86]. This of course raises the questions if i) the germ line cells correspond to
756 the pool of pluripotent stem cells involved in the regeneration process, or if ii) the
757 mesenteries contain in addition to the germ line, a pool of set aside stem cells that
758 respond to the amputation stress by migrating towards the wound site to reform missing
759 body parts. If the first idea would be true, then one would expect that a tradeoff between
760 sexual reproduction and regeneration might exist, as regeneration would exhaust the
761 germ-line pool for the tissue repair process. First experiments to analyze if sexual
762 reproduction is impaired after bisection, revealed that the spawning capacity of the

763 regenerated adult polyps remained unchanged (data not shown). While this suggests that
764 the germ line is different from the stem cell population in the mesenteries, additional
765 experiments are required to fully address this question.
766
767 Taken together, we provide a list of evidences that strongly support the idea that
768 there are at least two populations of stem cells in *Nematostella* that are actively deployed
769 and act in synergy during the regeneration process. However, further cellular (self-
770 renewal, potency) as well as molecular characterization (e.g. stem cell/pluripotency
771 markers) is needed in order to characterize in details their stem cell identity.
772
773 *The presence of mesenteries as specific feature of anthozoans may account for a spatial*
774 *dissociation of the signal-emitting and signal-receiving compartments required for*
775 *regeneration*
776 Hydrozoans lack mesenteries and their pluripotent stem cells (i-cells) are located
777 in the epithelia of the midgastric region and are able to give rise to the germ line as well
778 as somatic cells [87-89]. The present study revealed that anthozoans possess stem cell
779 populations that are located throughout the body within the epithelia but importantly also
780 within the mesenteries. Because the oocytes (germ line) are located within the
781 mesenteries, it is highly probable that, if any pluripotent stem cells (giving rise to germ
782 and soma) exist in *Nematostella* they are located within the mesenteries. Taken into an
783 evolutionary context one proposition would be that hydrozoans (*Hydra, Hydractinia*)
784 cope the lack of mesenteries with the existence of pluripotent stem cells (at the origin of
785 germ and somatic cells) as well as a regeneration-inducing signal localized both directly

786 within the epithelia. Our present results from the anthozoan sea anemone *Nematostella*
787 *vectensis* show that the regeneration signal emitting (mesenteries) and receiving
788 (epithelia) tissues are spatially separated and that a synergic effect of the stem cell
789 populations is required to complete the regeneration process. We thus propose that the
790 emergence/loss of structure complexity/compartmentalization can influence the
791 proprieties of tissue plasticity, changes the competence of tissues to reprogram and, in the
792 context of regeneration, the capacity to emit or respond to a regeneration-inducing signal.
793
794 **Conclusions**
795 Although cnidarian regeneration has intrigued scientists for over 300 years, little was
796 known about the origin of the regeneration inductive signal, the interplay between tissues
797 and its role on coordinating a particular cellular dynamics required for a successful
798 regeneration process. For the present study, we used *Nematostella vectensis,* an
799 anthozoan cnidarian that possesses promising features to become a potent and
800 complementary novel whole body regeneration model (reviewed in [44,90]). By
801 combining dissection and grafting experiments with functional and modern cellular
802 approaches we have identified i) the body structure that emits a regeneration inductive
803 signal, ii) the crucial importance of a tissue crosstalk to induce a cellular response and iii)
804 that two populations of stem cells, activated by the amputation stress and tissue crosstalk,
805 are synergically required to successfully complete the reformation of lost body parts. In
806 addition to the identification of the previously unknown anthozoan stem cell populations,
807 the tissue crosstalk we describe here has never been reported from other cnidarians. This
808 is mainly due to differences observed in cnidarian anatomies and opens new opportunities

809 to understand how the emergence/loss of structure complexity/compartmentalization can
810 influence the proprieties of the tissue plasticity that compose the body of an animal. This
811 in turn may have important implications on the competence of a tissue to reprogram and,
812 in the context of regeneration, the capacity to emit or respond to a regeneration-inducing
813 signal.
814
815

Acknowledgements

The authors thank the current team members as well as the Saccani, Liti, Shkreli and Féral labs for stimulating discussions on the project. We are grateful to Marina Shkreli for careful reading and comments on the manuscript. We also thank Isabelle Bourget for running the irradiation device and the Pasteur-IRCAN Molecular and Cellular Imaging Core Facility (PICMI) for providing access to the Zeiss LSM Exciter confocal microscope. PICMI was supported financially by: le Cancéropole PACA, la Région Provence Alpes-Côte d'Azur, le Conseil Départemental 06 and l'INSERM.

Funding

This project was funded by an ATIP-Avenir award (CNRS/INSERM/Plan Cancer), a Marie-Curie Career Integration Grant (CIG # 631665 – FP7 European Commission) and a "Fondation ARC pour la Recherche sur le Cancer" grant (# 20141201869) to ER, a FRM fellowship (Fondation pour la Recherche Médicale) to ARA and a Région PACA/INSERM fellowship to KF. The funders had no role in study design, data collection and analysis, decision to publish, or preparation of the manuscript.

Availability of data and materials

All biological material presented in this study is available upon request.

Authors' contributions

ARA and ER conceived and designed experiments. ARA, KF and SF performed experiments, generated, collected and analyzed data. ER contributed reagents, materials,

839 and analysis tools. ARA and ER drafted the manuscript. All authors read and approved
840 the final manuscript.

841

842 **Competing interests**

843 The authors declare that no competing interests exist

844

References

1. King RS, Newmark PA. Beyond the cell: The cell biology of regeneration. The Journal of Cell Biology. 2012;196:553–62.

2. Trembley A. Mémoires pour servir à l'histoire d'un genre de polypes d'eau douce, à bras en forme de cornes. Verbeek JH, editor. Leiden; 1744;:1–404.

3. Réaumur RA. Animaux coupés et partagés en plusieurs parties, et qui se reproduisent tout entiers dans chacune. (null), editor. Memoires de lAcademie Royale des Sciences de Paris. 1741;:33–5.

4. Sánchez Alvarado A, Tsonis PA. Bridging the regeneration gap: genetic insights from diverse animal models. Nat Rev Genet. 2006;7:873–84.

5. Galliot B, Schmid V. Cnidarians as a model system for understanding evolution and regeneration. Int J Dev Biol. 2002;46:39–48.

6. Holstein TW, Hobmayer E, Technau U. Cnidarians: an evolutionarily conserved model system for regeneration? Dev Dyn. 2003;226:257–67.

7. Bely AE, Nyberg KG. Evolution of animal regeneration: re-emergence of a field. Trends Ecol Evol (Amst). 2010;25:161–70.

8. Pallas PS. **Fasciola Punctata**. Spicilegia zoologica - Quibus novae imprimis et obscurae animalium species iconibus, descriptionibus atque comentariis illustrantur. 1774;:22–3.

9. Morgan TH. Experimental studies of the regeneration of Planaria maculata. Archiv für Entwickelungsmechanik der Organismen. Springer-Verlag; 1898;7:364–97.

10. Reddien PW, Alvarado AS. Fundamentals of planarian regeneration. Annu Rev Cell Dev Biol. 2004;20:725–57.

11. Wenemoser D, Reddien PW. Planarian regeneration involves distinct stem cell responses to wounds and tissue absence. Dev Biol. 2010;344:979–91.

12. David CN, Plotnick I. Distribution of interstitial stem cells in Hydra. Dev Biol. 1980;76:175–84.

13. Bode HR. Head regeneration inHydra. Dev Dyn. 2003;226:225–36.

14. Hazen AP. Regeneration in Hydractinia and Podocoryne. American Naturalist. 1902.

15. Schmid V, Schmid B, Schneider B, Stidwill R, Baker G. Factors effecting manubrium-regeneration in hydromedusae (Coelenterata). Wilhelm Roux' Archiv. Springer-Verlag; 1976;179:41–56.

16. Duffy DJ, Plickert G, Kuenzel T, Tilmann W, Frank U. Wnt signaling promotes oral but suppresses aboral structures in Hydractinia metamorphosis and regeneration. Development (Cambridge, England). 2010;137:3057–66.

17. Frank U, Leitz T, Müller WA. The hydroid Hydractinia: a versatile, informative cnidarian representative. Bioessays. John Wiley & Sons, Inc; 2001;23:963–71.

18. Marcum BA, Campbell RD. Development of Hydra lacking nerve and interstitial cells. J Cell Sci. 1978;29:17–33.

19. Galliot B. Regeneration in Hydra. eLS. Chichester, UK: John Wiley & Sons, Ltd; 2013.

20. Chera S, Ghila L, Dobretz K, Wenger Y, Bauer C, Buzgariu W, et al. Apoptotic Cells Provide an Unexpected Source of Wnt3 Signaling to Drive Hydra Head Regeneration. Dev Cell. Elsevier Ltd; 2009;17:279–89.

21. Gahan JM, Bradshaw B, Flici H, Frank U. The interstitial stem cells in Hydractinia and their role in regeneration. Curr Opin Genet Dev. 2016;40:65–73.

22. Bradshaw B, Thompson K, Frank U. Distinct mechanisms underlie oral versus aboral regeneration in the cnidarian Hydractinia echinata. eLife. 2015;4.

23. Müller WA, Teo R, Frank U. Totipotent migratory stem cells in a hydroid. Dev Biol. 2004;275:215–24.

24. Govindasamy N, Murthy S, Ghanekar Y. Slow-cycling stem cells in hydra contribute to head regeneration. Biology Open. 2014;3:1236–44.

25. Bridge D, Cunningham CW, Schierwater B, DeSalle R, Buss LW. Class-level relationships in the phylum Cnidaria: evidence from mitochondrial genome structure. Proceedings of the National Academy of Sciences. National Academy of Sciences; 1992;89:8750–3.

26. Kim J, Kim W, Cunningham CW. A new perspective on lower metazoan relationships from 18S rDNA sequences. Mol Biol Evol. 1999.

27. Medina M, Collins AG, Silberman JD, Sogin ML. Evaluating hypotheses of basal animal phylogeny using complete sequences of large and small subunit rRNA. Proceedings of the National Academy of Sciences. National Acad Sciences; 2001;98:9707–12.

28. Collins AG, Schuchert P, Marques AC, Jankowski T, Medina M, Schierwater B. Medusozoan phylogeny and character evolution clarified by new large and small subunit rDNA data and an assessment of the utility of phylogenetic mixture models. Syst. Biol. Oxford University Press; 2006;55:97–115.

29. Dunn CW, Hejnol A, Matus DQ, Pang K, Browne WE, Smith SA, et al. Broad

912 phylogenomic sampling improves resolution of the animal tree of life. Nature. Nature
913 Publishing Group; 2008;452:745–9.

914 30. Philippe H, Derelle R, Lopez P, Pick K, Borchiellini C, Boury-Esnault N, et al.
915 Phylogenomics revives traditional views on deep animal relationships. Curr Biol.
916 2009;19:706–12.

917 31. Erwin DH. Wonderful Ediacarans, wonderful cnidarians? Evol Dev. Blackwell
918 Publishing Inc; 2008;10:263–4.

919 32. Gold DA, Jacobs DK. Stem cell dynamics in Cnidaria: are there unifying principles?
920 Dev Genes Evol. 2012;223:53–66.

921 33. Zapata F, Goetz FE, Smith SA, Howison M, Siebert S, Church SH, et al.
922 Phylogenomic Analyses Support Traditional Relationships within Cnidaria. Steele RE,
923 editor. PLoS ONE. Public Library of Science; 2015;10:e0139068.

924 34. Daly M, Brugler MR, Cartwright P, Collins AG. The phylum Cnidaria: a review of
925 phylogenetic patterns and diversity 300 years after Linnaeus. 2007.

926 35. Zhang ZQ. Animal biodiversity: An introduction to higher-level classification and
927 taxonomic richness. Zootaxa. 2011.

928 36. Fautin D, Mariscal R. Microscopic anatomy of invertebrates: Anthozoa. Harrison FW,
929 Ruppert EE, editors. 1991;:1–93.

930 37. Won J, Rho B, Song J. A phylogenetic study of the Anthozoa (phylum Cnidaria)
931 based on morphological and molecular characters. Coral reefs. Springer-Verlag;
932 2001;20:39–50.

933 38. Babonis LS, Martindale MQ, Ryan JF. Do novel genes drive morphological novelty?
934 An investigation of the nematosomes in the sea anemone Nematostella vectensis. BMC
935 Evol Biol. BMC Evolutionary Biology; 2016;16:1–22.

936 39. Hand C, Uhlinger KR. The culture, sexual and asexual reproduction, and growth of
937 the sea anemone Nematostella vectensis. Biol Bull. MBL; 1992;182:169–76.

938 40. Fritzenwanker JH, Technau U. Induction of gametogenesis in the basal cnidarian
939 Nematostella vectensis (Anthozoa). Dev Genes Evol. 2002;212:99–103.

940 41. Stefanik DJ, Friedman LE, Finnerty JR. Collecting, rearing, spawning and inducing
941 regeneration of the starlet sea anemone, Nematostella vectensis. Nat Protoc. 2013;8:916–
942 23.

943 42. Putnam NH, Srivastava M, Hellsten U, Dirks B, Chapman J, Salamov A, et al. Sea
944 anemone genome reveals ancestral eumetazoan gene repertoire and genomic organization.
945 Science. 2007;317:86–94.

946 43. Layden MJ, Röttinger E, Wolenski FS, Gilmore TD, Martindale MQ. Microinjection
947 of mRNA or morpholinos for reverse genetic analysis in the starlet sea anemone,
948 Nematostella vectensis. Nat Protoc. 2013;8:924–34.

949 44. Layden MJ, Rentzsch F, Röttinger E. The rise of the starlet sea anemone
950 Nematostella vectensis as a model system to investigate development and regeneration.
951 WIREs Dev Biol. John Wiley & Sons, Inc; 2016.

952 45. Ikmi A, McKinney SA, Delventhal KM, Gibson MC. TALEN and CRISPR/Cas9-
953 mediated genome editing in the early-branching metazoan Nematostella vectensis. Nature
954 Communications. 2014;5:5486.

955 46. Kusserow A, Pang K, Sturm C, Lentfer J, Schmidt HA, Technau U, et al. Unexpected
956 complexity of the Wnt gene family in a sea anemone. Nature. 2005;433:156–60.

957 47. Schwaiger M, Schonauer A, Rendeiro AF, Pribitzer C, Schauer A, Gilles AF, et al.
958 Evolutionary conservation of the eumetazoan gene regulatory landscape. Genome
959 Research. 2014.

960 48. Rentzsch F, Fritzenwanker JH, Scholz CB, Technau U. FGF signalling controls
961 formation of the apical sensory organ in the cnidarian Nematostella vectensis.
962 Development. 2008;135:1761–9.

963 49. Saina M, Technau U. Characterization of myostatin/gdf8/11 in the starlet sea
964 anemone Nematostella vectensis. J Exp Zool. 2009.

965 50. Layden MJ, Boekhout M, Martindale MQ. Nematostella vectensis achaete-scute
966 homolog NvashA regulates embryonic ectodermal neurogenesis and represents an ancient
967 component of the metazoan neural specification pathway. Development (Cambridge,
968 England). 2012;139:1013–22.

969 51. Röttinger E, Dahlin P, Martindale MQ. A Framework for the Establishment of a
970 Cnidarian Gene Regulatory Network for "Endomesoderm" Specification: The Inputs of
971 ß-Catenin/TCF Signaling. Mullins MC, editor. PLoS Genet. 2012;8:e1003164.

972 52. Leclère L, Rentzsch F. RGM Regulates BMP-Mediated Secondary Axis Formation in
973 the Sea Anemone Nematostella vectensis. CellReports. 2014;9:1921–30.

974 53. Layden MJ, Johnston H, Amiel AR, Havrilak J, Steinworth B, Chock T, et al. MAPK
975 signaling is necessary for neurogenesis in Nematostella vectensis. BMC Biol. 2016;14:61.

976 54. Genikhovich G, Fried P, Prünster MM, Schinko JB, Gilles AF, Fredman D, et al.
977 Axis Patterning by BMPs: Cnidarian Network Reveals Evolutionary Constraints.
978 CellReports. 2015;10:1646–54.

979 55. Wikramanayake AH, Hong M, Lee PN, Pang K, Byrum CA, Bince JM, et al. An
980 ancient role for nuclear beta-catenin in the evolution of axial polarity and germ layer
981 segregation. Nature. 2003;426:446–50.

982 56. Burton PM, Finnerty JR. Conserved and novel gene expression between regeneration
983 and asexual fission in Nematostella vectensis. Dev Genes Evol. 2009;219:79–87.

984 57. Tucker RP, Shibata B, Blankenship TN. Ultrastructure of the mesoglea of the sea
985 anemone Nematostella vectensis (Edwardsiidae). Invertebrate Biology. 2011;130:11–24.

986 58. Trevino M, Stefanik DJ, Rodriguez R, Harmon S, Burton PM. Induction of canonical
987 Wnt signaling by alsterpaullone is sufficient for oral tissue fate during regeneration and
988 embryogenesis in Nematostella vectensis. Dev Dyn. 2011;240:2673–9.

989 59. Passamaneck YJ, Martindale MQ. Cell proliferation is necessary for the regeneration
990 of oral structures in the anthozoan cnidarian Nematostella vectensis. BMC Dev Biol.
991 BMC Developmental Biology; 2012;12:1–1.

992 60. Bossert PE, Dunn MP, Thomsen GH. A staging system for the regeneration of a
993 polyp from the aboral physa of the anthozoan cnidarian *Nematostella vectensis*. Dev Dyn.
994 2013;242:1320–31.

995 61. Schaffer AA, Bazarsky M, Levy K, Chalifa-Caspi V, Gat U. A transcriptional time-
996 course analysis of oral vs. aboral whole-body regeneration in the Sea anemone
997 Nematostella vectensis. BMC Genomics. 2016;17:718.

998 62. Amiel AR, Johnston HT, Nedoncelle K, Warner JF, Ferreira S, Röttinger E.
999 Characterization of Morphological and Cellular Events Underlying Oral Regeneration in
1000 the Sea Anemone, Nematostella vectensis. Int J Mol Sci. 2015;16:28449–71.

1001 63. Ormestad M, Amiel A, Röttinger E. Ex-situ Macro Photography of Marine Life.
1002 Imaging Marine Life. Weinheim, Germany: Wiley-VCH Verlag GmbH & Co. KGaA;
1003 2013. pp. 210–33.

1004 64. Cheung TH, Rando TA. Molecular regulation of stem cell quiescence. Nat Rev Mol
1005 Cell Biol. 2013;14:329–40.

1006 65. Bickenbach JR. Identification and behavior of label-retaining cells in oral mucosa and
1007 skin. J. Dent. Res. 1981;60 Spec No C:1611–20.

1008 66. Morris RJ, Fischer SM, Slaga TJ. Evidence that the centrally and peripherally located
1009 cells in the murine epidermal proliferative unit are two distinct cell populations. Journal
1010 of Investigative Dermatology. 1985;84:277–81.

1011 67. Braun KM, Watt FM. Epidermal label-retaining cells: background and recent
1012 applications. J. Investig. Dermatol. Symp. Proc. 2004;9:196–201.

1013 68. Zhang L, Li H, Zeng S, Chen L, Fang Z, Huang Q. Long-term tracing of the BrdU
1014 label-retaining cells in adult rat brain. Neurosci. Lett. 2015;591:30–4.

1015 69. Nemeth K, Karpati S. Identifying the Stem Cell. Journal of Investigative
1016 Dermatology. Elsevier Masson SAS; 2014;134:1–5.

1017 70. Ishizuya-Oka A. Epithelial-connective tissue cross-talk is essential for regeneration of
1018 intestinal epithelium. J Nippon Med Sch. 2005;72:13–8.

1019 71. Lemons ML, Condic ML. Integrin signaling is integral to regeneration. Experimental
1020 Neurology. 2008;209:343–52.

1021 72. Satoh A, Makanae A, Hirata A, Satou Y. Blastema induction in aneurogenic state and
1022 Prrx-1 regulation by MMPs and FGFs in Ambystoma mexicanum limb regeneration. Dev
1023 Biol. 2011;355:263–74.

1024 73. Makanae A, Satoh A. Early regulation of axolotl limb regeneration. Anat Rec
1025 (Hoboken). Wiley Subscription Services, Inc., A Wiley Company; 2012;295:1566–74.

1026 74. Monaghan JR, Athippozhy A, Seifert AW, Putta S, Stromberg AJ, Maden M, et al.
1027 Gene expression patterns specific to the regenerating limb of the Mexican axolotl.
1028 Biology Open. 2012;1:937–48.

1029 75. Endo T, Bryant SV, Gardiner DM. A stepwise model system for limb regeneration.
1030 Dev Biol. 2004;270:135–45.

1031 76. Wernig F, Mayr M, Xu Q. Mechanical stretch-induced apoptosis in smooth muscle
1032 cells is mediated by beta1-integrin signaling pathways. Hypertension. Lippincott
1033 Williams & Wilkins; 2003;41:903–11.

1034 77. Fujisawa T. Role of interstitial cell migration in generating position-dependent
1035 patterns of nerve cell differentiation in Hydra. Dev Biol. 1989;133:77–82.

1036 78. Boehm A-M, Bosch TCG. Migration of multipotent interstitial stem cells in Hydra.
1037 Zoology (Jena). 2012;115:275–82.

1038 79. Mochizuki K, Sano H, Kobayashi S, Nishimiya-Fujisawa C, Fujisawa T. Expression
1039 and evolutionary conservation of nanos-related genes in Hydra. Dev Genes Evol.
1040 2000;210:591–602.

1041 80. Rebscher N, Volk C, Teo R, Plickert G. The germ plasm component Vasa allows
1042 tracing of the interstitial stem cells in the cnidarian Hydractinia echinata. Dev Dyn.
1043 Wiley-Liss, Inc; 2008;237:1736–45.

1044 81. Gustafson EA, Wessel GM. Vasa genes: emerging roles in the germ line and in
1045 multipotent cells. Bioessays. WILEY-VCH Verlag; 2010;32:626–37.

1046 82. Alié A, Leclère L, Jager M, Dayraud C, Chang P, Le Guyader H, et al. Somatic stem
1047 cells express Piwi and Vasa genes in an adult ctenophore: Ancient association of
1048 "germline genes" with stemness. Dev Biol. Elsevier Inc; 2011;350:183–97.

1049 83. Plickert G, Frank U, Müller WA. Hydractinia, a pioneering model for stem cell
1050 biology and reprogramming somatic cells to pluripotency. Int J Dev Biol. 2012;56:519–
1051 34.

1052 84. Alié A, Hayashi T, Sugimura I, Manuel M, Sugano W, Mano A, et al. The ancestral
1053 gene repertoire of animal stem cells. Proc Natl Acad Sci USA. 2015;112:E7093–100.

1054 85. Rinkevich B, Matranga V. Stem Cells in Marine Organisms. Springer Verlag; 2009.

1055 86. Extavour CG, Pang K, Matus DQ, Martindale MQ. vasa and nanos expression
1056 patterns in a sea anemone and the evolution of bilaterian germ cell specification
1057 mechanisms. Evol Dev. 2005;7:201–15.

1058 87. Bode HR. The interstitial cell lineage of hydra: a stem cell system that arose early in
1059 evolution. J Cell Sci. 1996.

1060 88. Bosch TCG, Anton-Erxleben F, Hemmrich G, Khalturin K. The Hydra polyp: nothing
1061 but an active stem cell community. Dev Growth Differ. 2010;52:15–25.

1062 89. Galliot B, Ghila L. Cell plasticity in homeostasis and regeneration. Mol. Reprod. Dev.
1063 Wiley Subscription Services, Inc., A Wiley Company; 2010;77:837–55.

1064 90. Leclère L, Röttinger E. Diversity of cnidarian muscles: function, anatomy,
1065 development and regeneration. Front Cell Dev Biol. Frontiers; 2017;4:E3365.

1066

1067

Figures and Figure legends

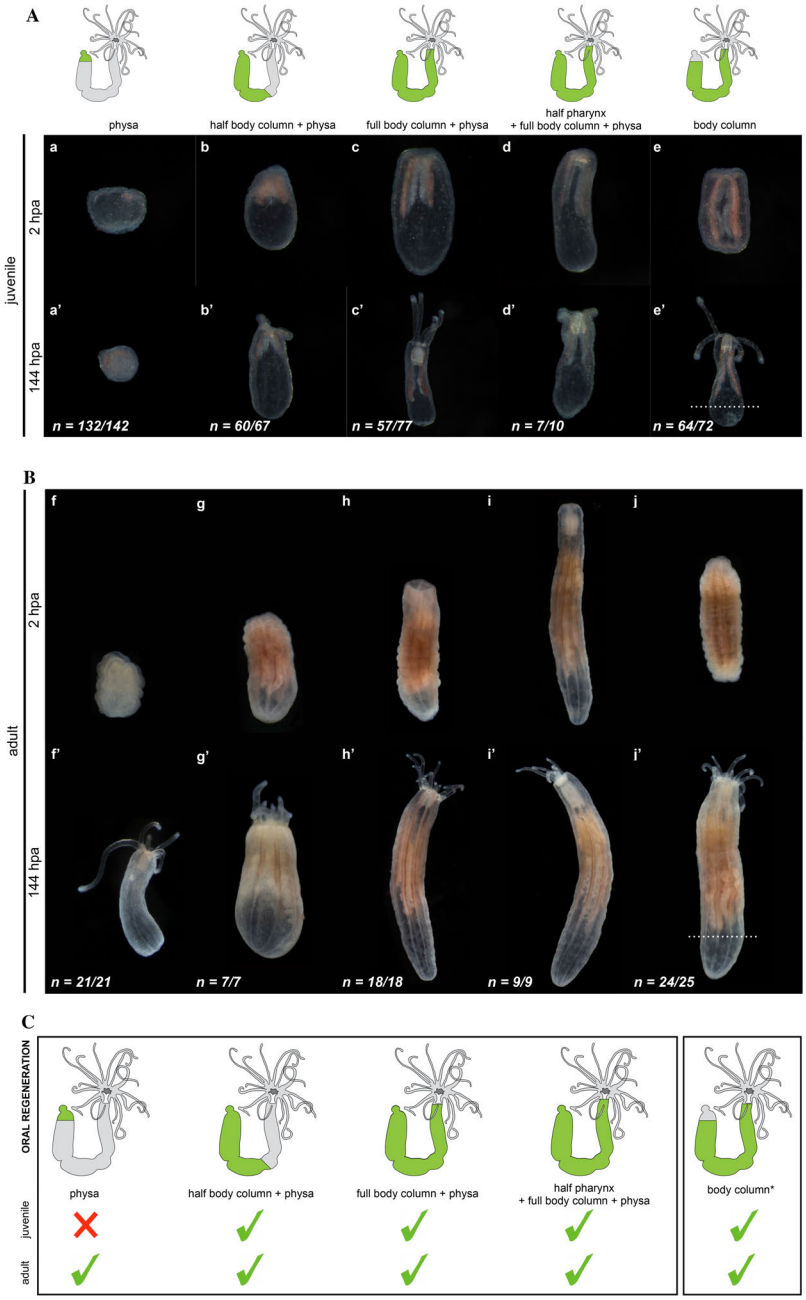

Figure 1. Oral regenerative capacity analyzed in juveniles (Aa-e, Aa'-e') and adults (Bf-j, Bf'-j') from isolated [physa] (Aa, Aa', Bf, Bf'); [half body column + physa] (Ab, Ab', Bg, Bg'); [full body column + physa] (Ac, Ac', Bh, Bh'); [half pharynx + full body column + physa] (Ad, Ad', Bi, Bi'); [body column] (Ae, Ae', Bj, Bj') from which aboral regeneration was also assessed (dashed line in Ae', Bj'). On top of each panel are *Nematostella* illustrations in which each isolated part is indicated in green and the part scored for regeneration in grey. Photographs of the isolated body parts at 2hpa (Aa-e, Bf-j). Phenotypes observed after 144hpa (6 days post amputation) (Aa'-e', Bf'-j'). n=[number of specimen with represented phenotype]/[total number of analyzed specimen]. **C**. Diagram summarizing the oral regeneration experiments carried out in juveniles and adults. Green parts in the schematic *Nematostella* indicate the isolated body part, green checkmarks regenerative success and red crosses the absence of regeneration after body part isolation.

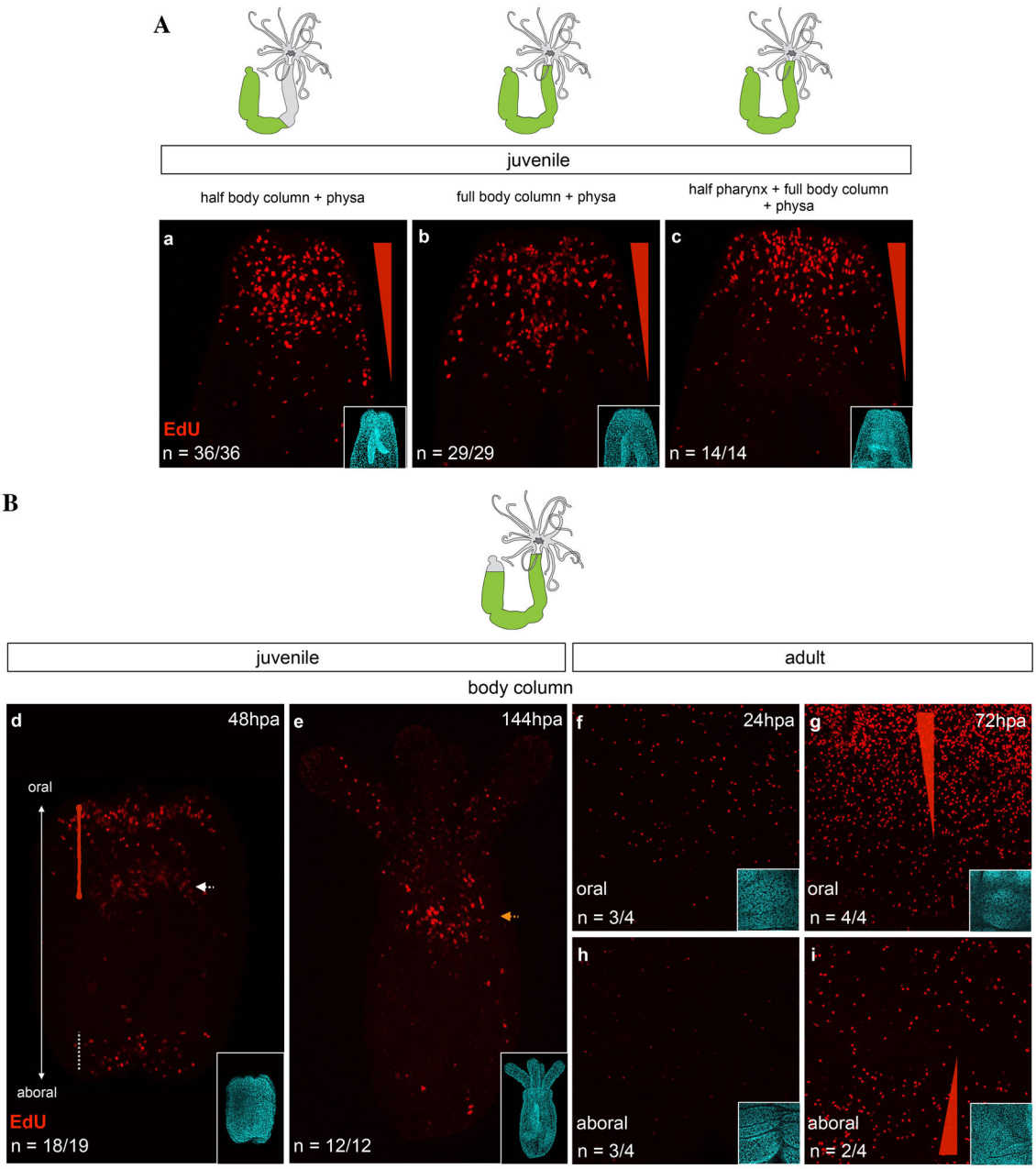

Figure 2. A. Cell proliferation in juveniles at 48hpa for [half body column + physa] (a), [full body column + physa]](b) and [half pharynx + full body column + physa] (c). **B**. Cell proliferation in juveniles at 48 (d) and 144hpa (e) and in adult at 24 (f, oral; h, aboral) and 72hpa (g, oral; i, aboral) for [body column]. The left red triangle in g and i represent a gradient of cell proliferation. Confocal images of cell proliferation in red (EdU) (Aa-c, Bd-i) and DNA/nucleus in cyan (DAPI) (small insert in Aa-c, Bd-i). n=[number of specimen with represented phenotype]/[total number of analyzed specimen].

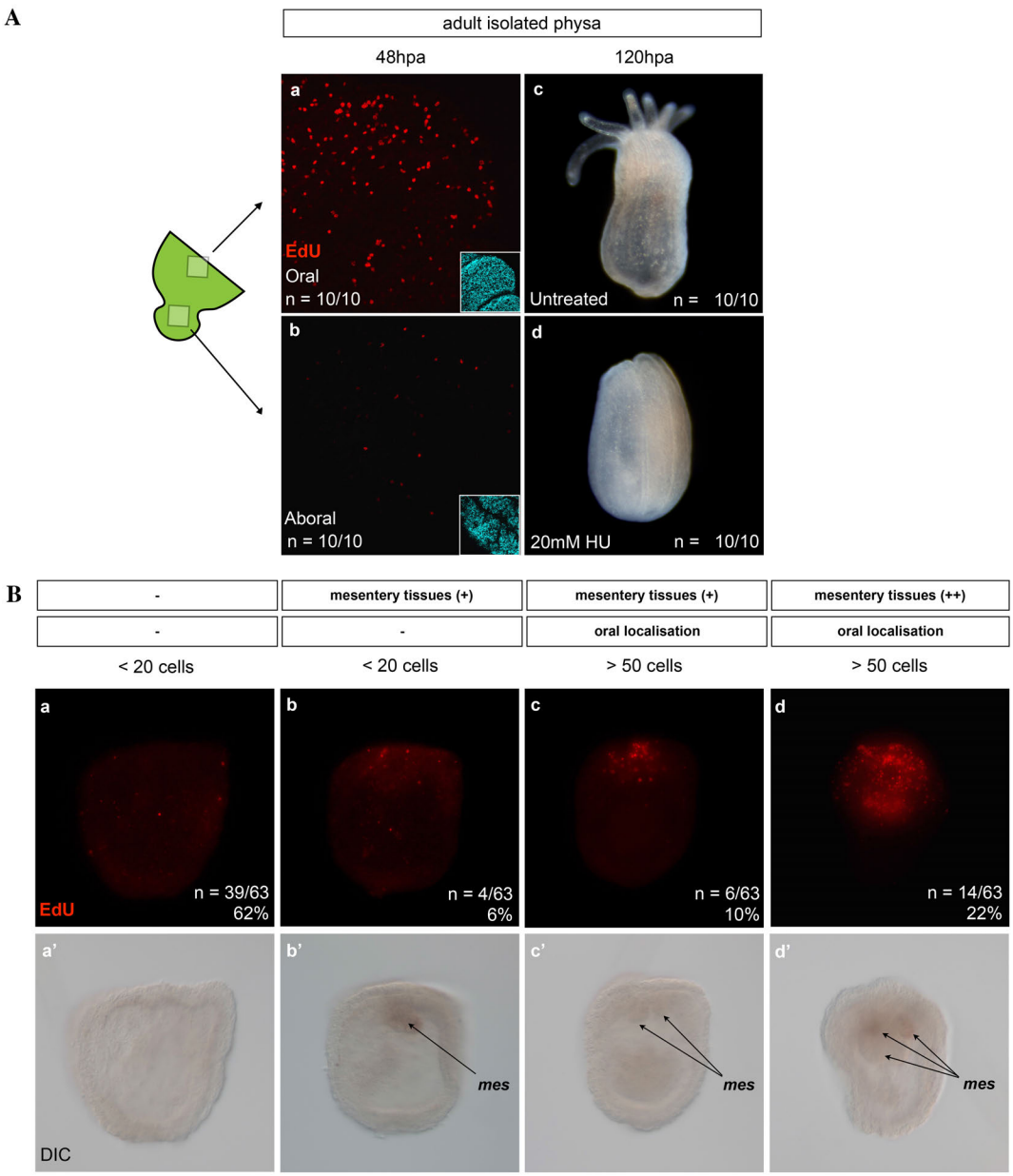

Figure 3. Cell proliferation in adult (**A**) and juvenile (**B**) [physa]. **A**. In adults, cell proliferation is present at the amputation site (Aa,b) and required for regeneration (c,d) of the [physa]. (a,b) Confocal microscopy images showing cellular proliferation in red (EdU) at 48hpa (a,b). Oral most part (a) and aboral most part (b) of the adult isolated physa. The cartoon to the left indicates the isolated physa and the regions represented in (a) and (b). (c,d) Hydroxyurea (HU) at 20mM was used in this set of experiment to inhibit cell proliferation in adult [physa] (untreated control in c, HU treated animal in d). n=[number of specimen with represented phenotype]/[total number of analyzed specimen]. **B**. Cell proliferation is absent/reduced in isolated juvenile physa at 48hpa. Observation of cellular proliferation at 48hpa using EdU staining on isolated juvenile physa. (a-d) Fluorescence microscopy images showing cellular proliferation (green), (a'-d') corresponding DIC images of the isolated physa represented above. Black arrows indicate the position of remaining mesentery tissue. On top of the panel the number of EdU positive cells (< 20 cells to > 50 cells), the amount of mesentery tissue (-, absent, +, few or ++, more than few) as well as the localization of EdU staining (-, random, oral) within the isolated physa are represented. n=[number of specimen with represented phenotype]/[total number of analyzed specimen]

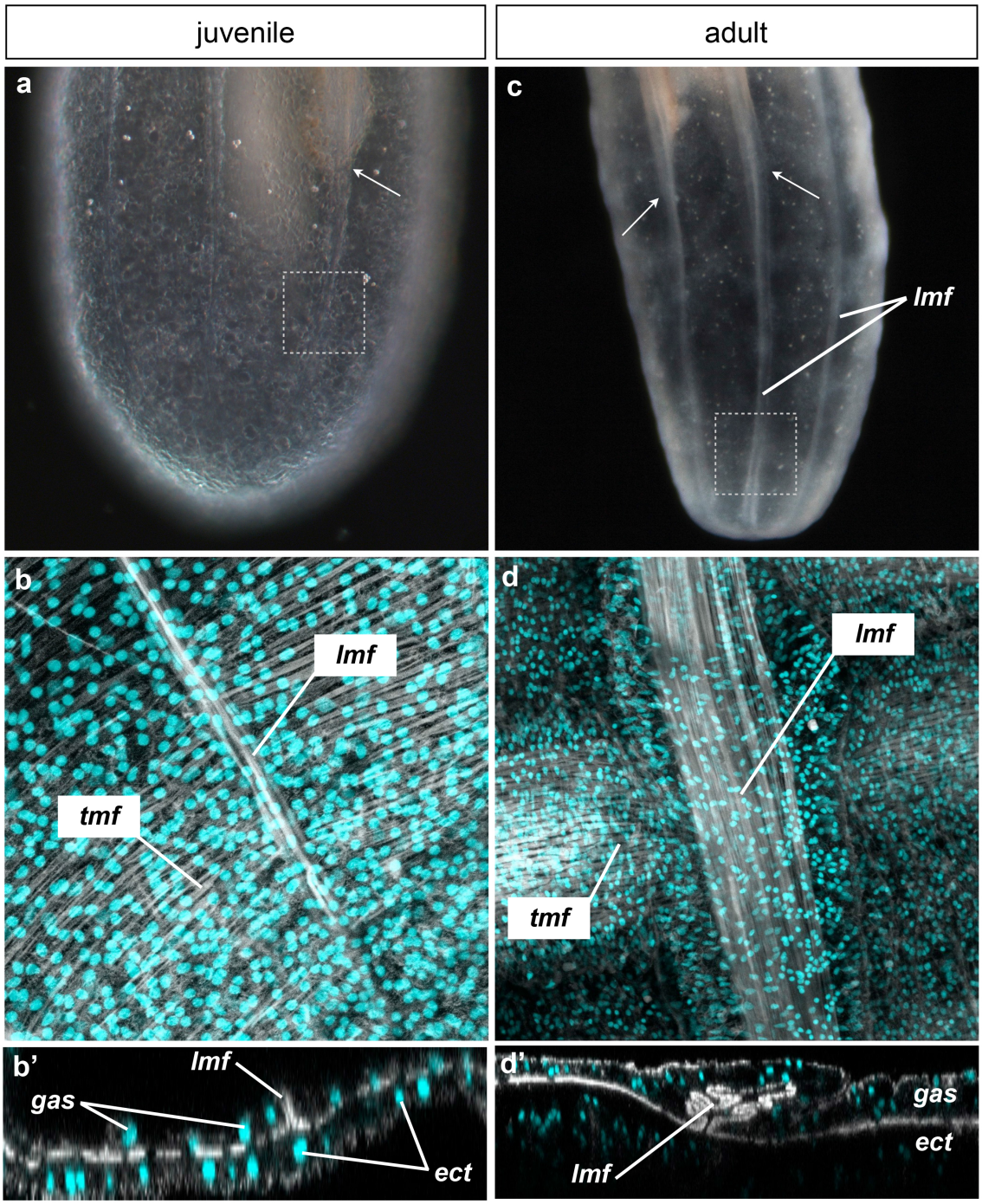

Figure 4. Comparison of the physa anatomy between juvenile (a, b, b') and adult (c, d, d'). (a) and (c) are macrophotographs. (b, b', d, d') are confocal stack images in which the DNA (nucleus) is labeled with DAPI (cyan), and the actin microfilaments (muscle fibers and cell membranes) are labeled with PhallAcidin (white). These confocal stack images are close-ups of the physa where longitudinal muscle fibers are present. (b') and (d') are orthogonal confocal projection of the stacks (b) and (d), respectively. White arrows indicate either the end (a) or the continuity (c) of the mesenteries. Dashed squares in (a) and (c) indicate the region represented in (b) and (d) respectively. *ect*, ectoderme; *gas*, gastrodermis; *lmf*, longitudinal muscle fibers; *tmf*, transversal muscle fibers.

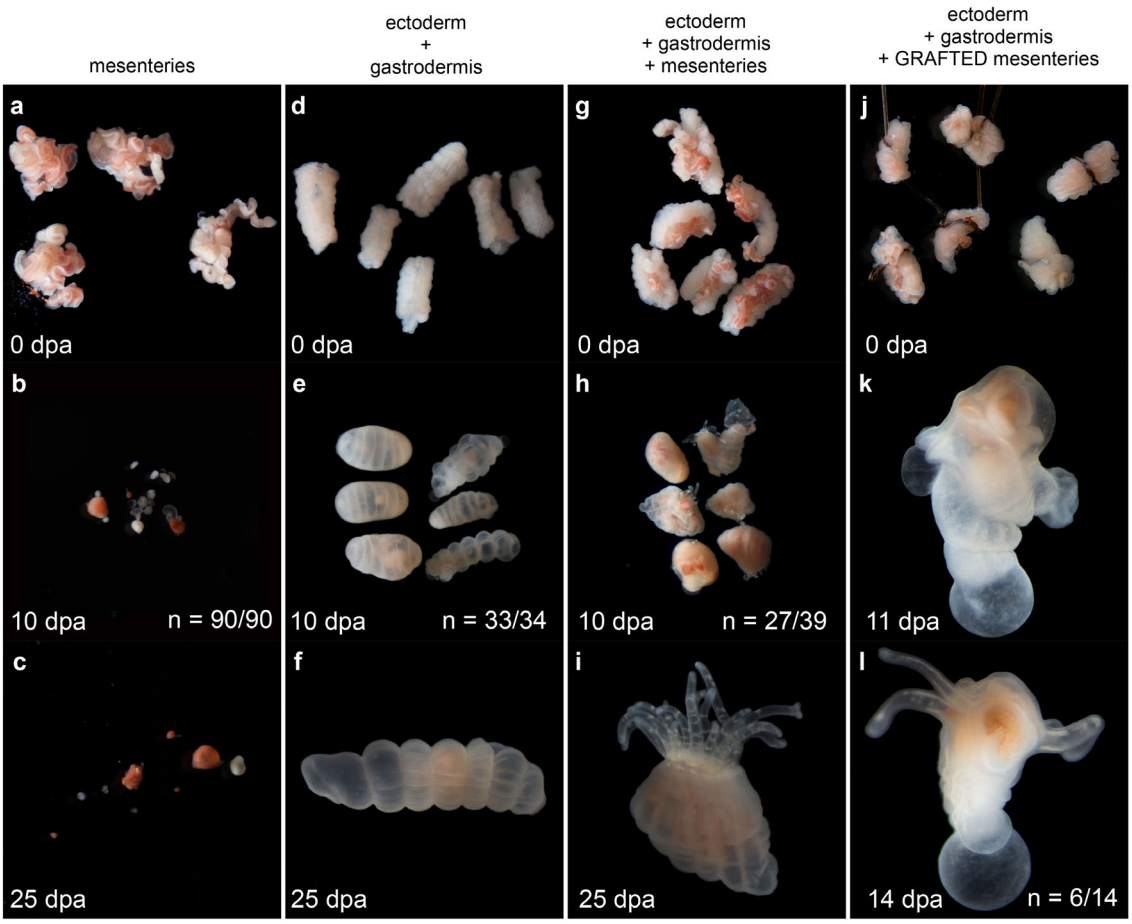

Figure *5*. Mesenteries are required for regeneration. Regenerative success was assayed after tissue isolation experiments in which mesenteries were isolated from the ectodermal and gastrodermal epithelia. The isolated tissues or the type of grafting experiment is indicated on top of the panel. The time scale is from top to bottom of the figure and indicated in days post amputation (dpa) in the left bottom corner of each image. White numbers in (b, e, h, k, n) are the n=[number of specimen with represented phenotype]/[total number of analyzed specimen].

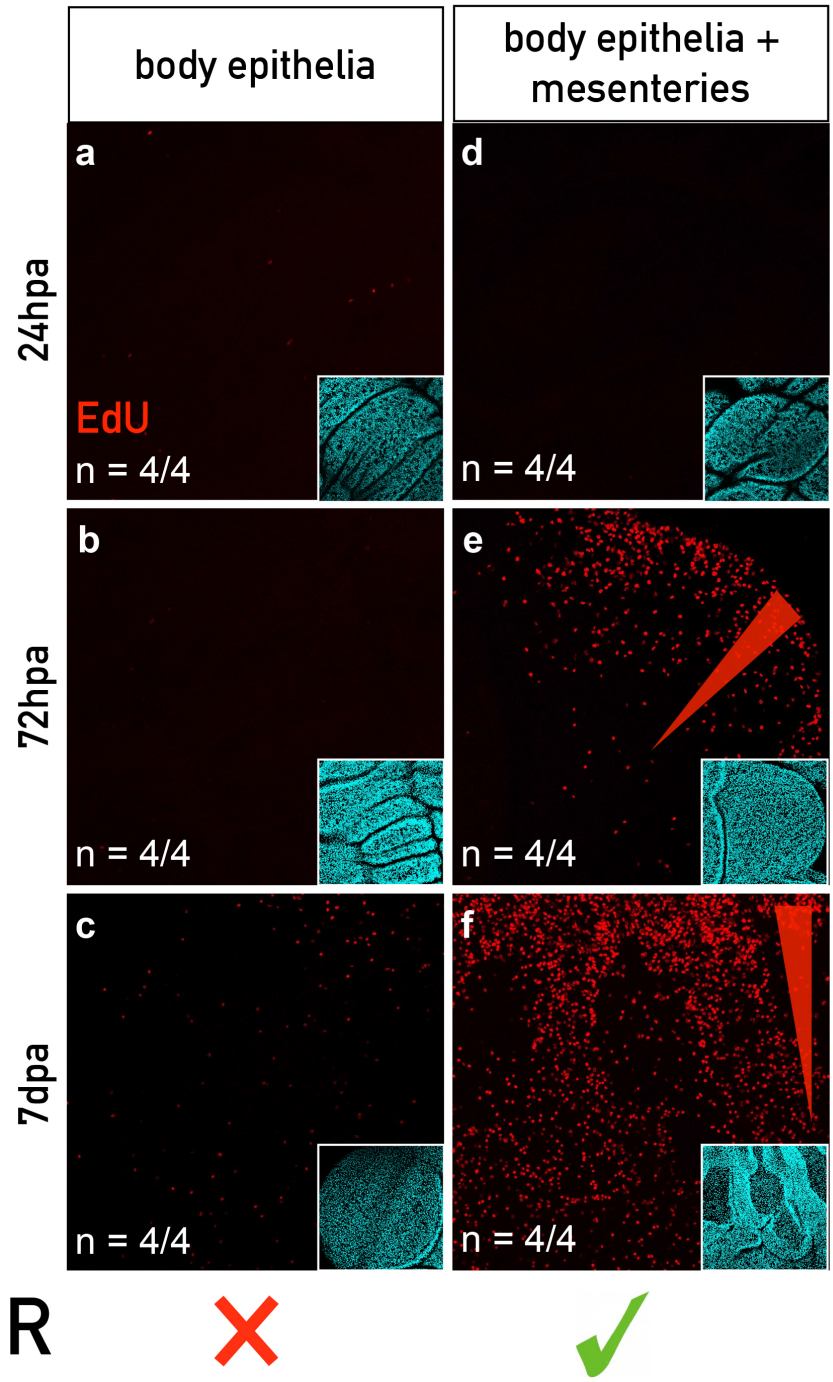

Figure 6. Mesenteries are required for cell proliferation during regeneration. Cell proliferation using EdU staining at various time point during regeneration in adult [body epithelia] (a-c, a'-c') and [body epithelia + mesenteries] (d-f, d'-f'). Confocal microscopy images showing cellular proliferation (a-f; red) and DAPI (a'-f'; cyan) for corresponding images. Red triangle in (e, f) indicates the gradient of proliferating cells at the regenerating site. No regeneration occurs in the [body epithelia] (a-c, a'-c') indicated by a red cross at the bottom of the panel in front of R (Regeneration). Regeneration occurs in the [body epithelia + mesenteries] (d-f, d'-f') indicated by a green check at the bottom of the panel in front of R (Regeneration). n=[number of specimen with represented phenotype]/[total number of analyzed specimen].

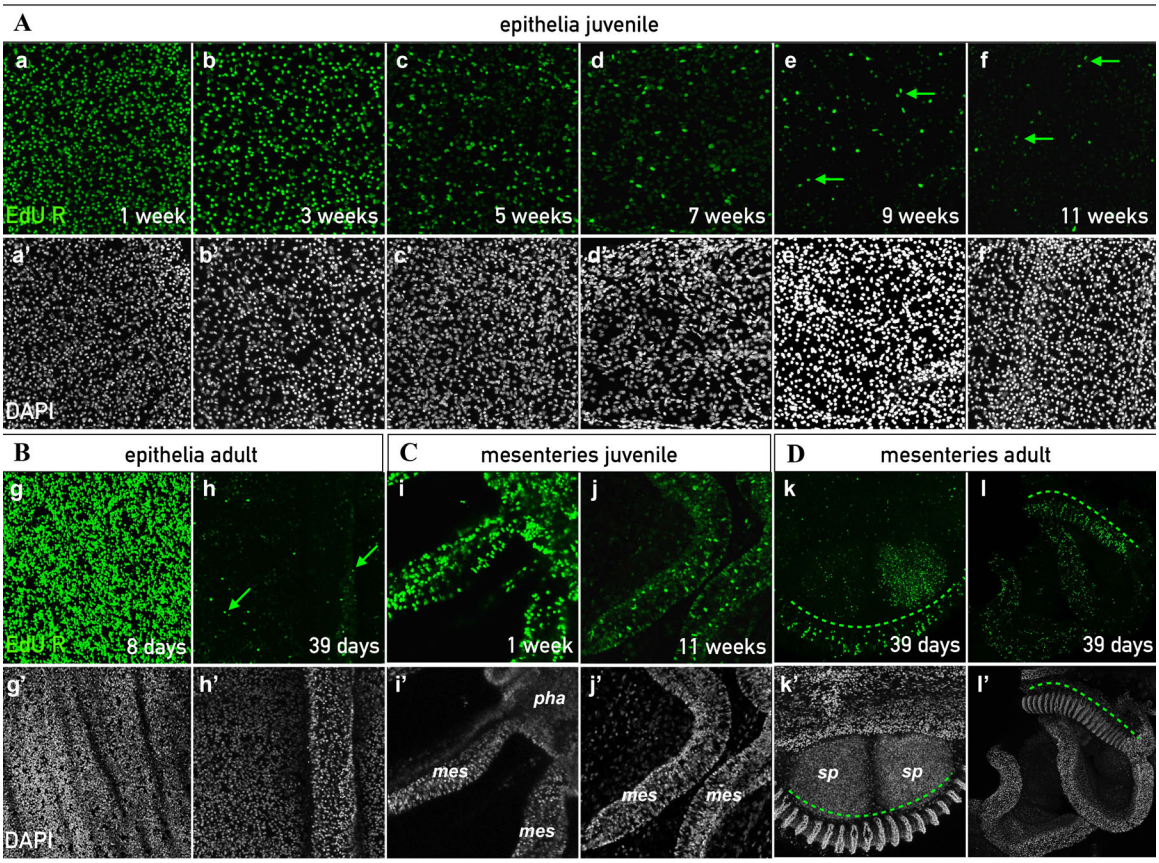

Figure 7. Presence of Label Retaining cells (LRCs) in uncut juveniles (A, D) and adults (B, C). **A**. LRCs present in juvenile epithelia that following a 1 week pulse, were chased at 1 (a,a'), 3 (b,b'), 5 (c,c'), 7 (d,d'), 9 (e,e'), and 11 weeks (f,f'). **B.** LRCs in adult epithelia chased at 7 (g,g') and 39 days (h,h') after a 1 week pulse. **C.** LRCs in juvenile mesenteries chased at 1 (i,i') and 11 weeks (j,j') after a 1 week pulse. **D.** LRCs in adult mesenteries chased at 39 days (k,k',l,l') after a 1 week pulse. LRCs are stained in green (a-l). Nuclei in white (DAPI) (a'-l'). Green arrows (d-h) and the discontinued line (k,k',l,l') indicate LRCs pairs and the zone of LRC accumulation in the gonad, respectively. *mes*, mesenteries; *pha*, pharynx; *sp*, sperm mass.

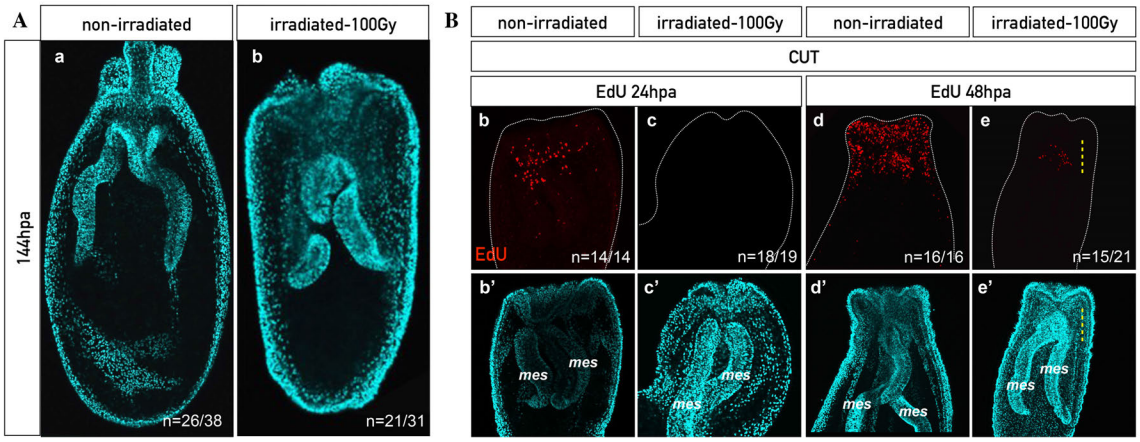

Figure 8. A. X-ray irradiation perturbs head regeneration. Confocal images of control non-irradiated (a) and X-ray irradiated (a') animal at 144hpa. Nuclei are in cyan (DAPI) (a, a'). **B.** A population of cells in the mesenteries is able to re-enter the mitotic cycle 48 hours post irradiation (hpirr). Confocal images of control non irradiated (b,b': 24hpa; d,d': 48hpa) and irradiated (c,c': 24hpa; e,e': 48hpa) polyps. A few cells in the mesenteries, localized at the amputation site, were able to re-enter the cell cycle between 24 and 48hpa (e, e'). EdU staining in red shows cell proliferation (b-e). Nuclei are in cyan (DAPI) (b'-e'). *mes*, mesenteries; *pha*, pharynx; *ten*, tentacles. n=[number of specimen with represented phenotype]/[total number of analyzed specimen].

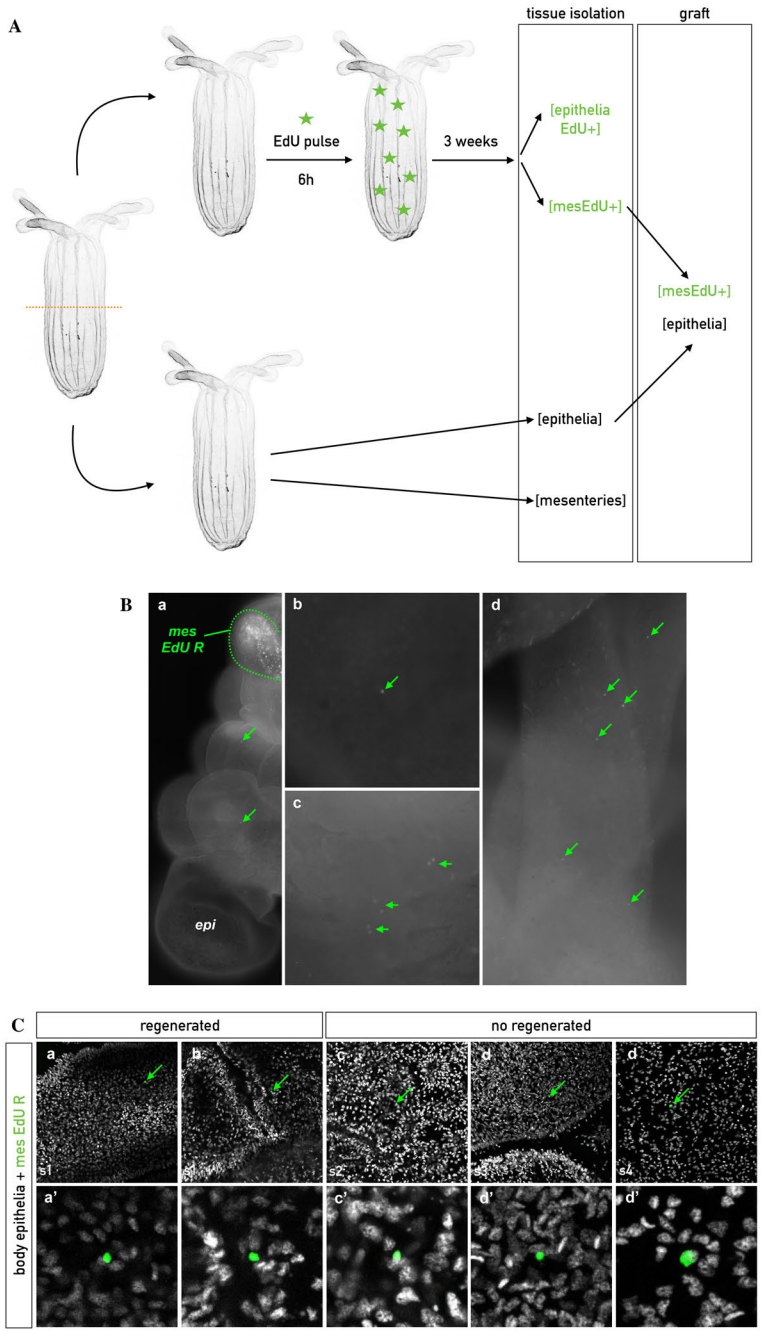

Figure 9. A. Diagram of the protocol to assess cell migration in graft experiments. [epithelia EdU+] and [mes EdU+] represent the isolated epithelia of the body wall and the mesenteries, respectively, that were labeled with EdU (from clone 1). [epithelia] and [mesenteries] represent the isolated epithelia of the body wall and the mesenteries, respectively, that were not labeled (from clone 2). **B.** Fluorescence imaging of the resulting graft experiments ([epithelia] + [mesLRC]). The discontinued green line indicates the position of the [mesLRC]) 14 days after being grafted into the [epithelia] (*epi*). Green arrows indicate EdU+ cells from the [mesLRC] that retained the EdU and migrated into the non labeled [epithelia] (a and b). In addition, they were able to divide as indicated by the presence of cell pairs (c) that can be localized in the regenerating tentacles (d). **C.** Confocal imaging of EdU+ cells from the [mesLRC] that retained EdU and migrated into the non labeled [epithelia]. Overlap of the nucleus staining in white (DAPI) and EdU R in green (a-d, a'-d'). a'-d' are magnification of the EdU+ cell from a-d.

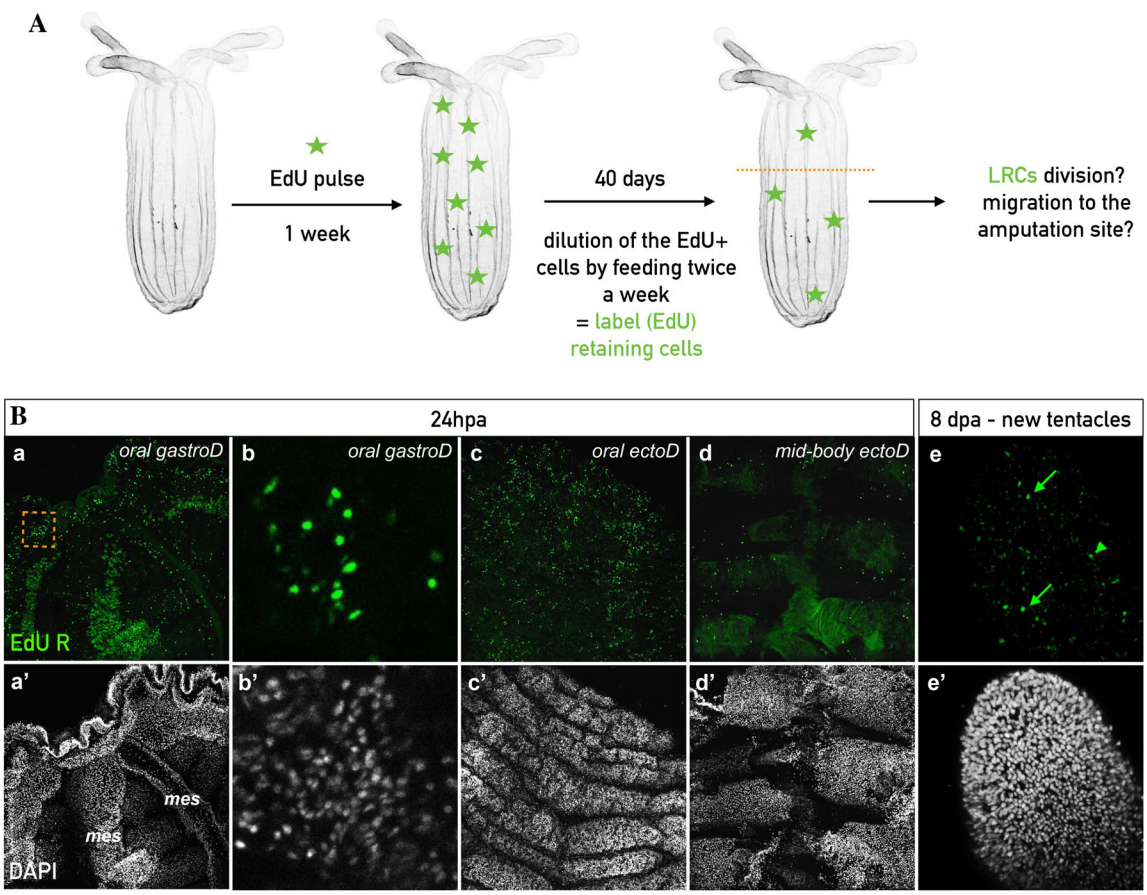

Figure 10. A. Diagram of the protocol assessing LRC dynamics during regeneration. After a one-week pulse with EdU, adult polyps were rinsed thoroughly with 1/3x seawater and kept for 40 days. Then, sub-pharyngeal amputation was performed and LRCs were chased at 24, 48 and 72hpa. **B**. Confocal imaging of LRC dynamics in regenerating polyps. LRCs are stained in green (a-e). Nuclei are in white (DAPI) (a'-e'). Regenerating adult polyps at 24hpa (a-d, a'-d'), accumulation of the LRCs cells is detected at the oral side (a,b,d) but not in the epithelia of the body wall (c). b and b' are the magnification of the square in (a) that indicate a cluster of LRCs at the amputation site during the regeneration process. LRCs are detected in the newly regenerated tentacles (e,e'; green arrows). *mes*, mesenteries; *mid-body ectoD*, mid-body region ectodermal view*; oral ectoD*, oral region ectodermal view*; oral gastroD*, oral region gastrodermal view.

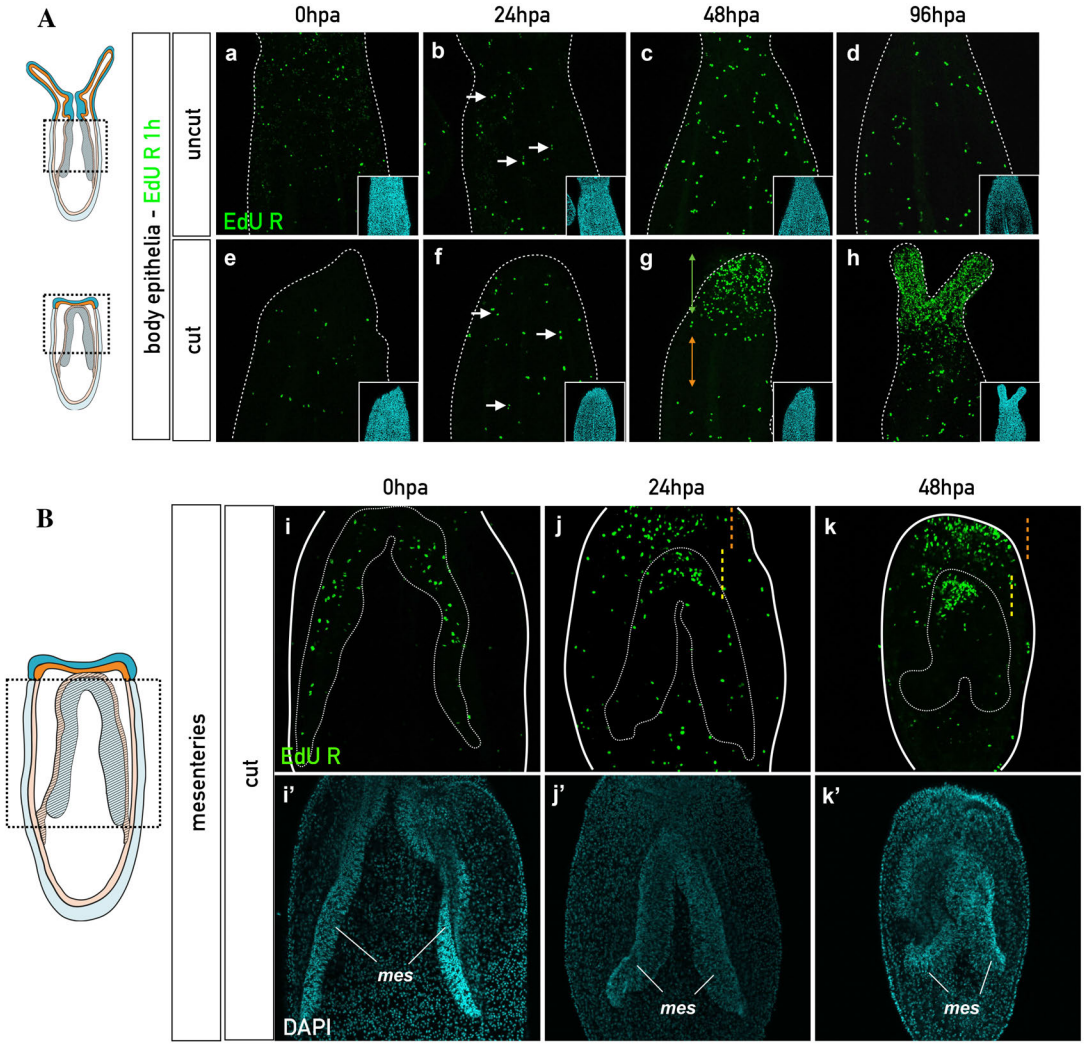

Figure 11. Accumulation of EdU+ cells at the amputation site during regeneration. Confocal images of the EdU "pulse-1h-and chase experiment" on uncut (epithelia: Aa-d) and cut (Epithelia: Ae-h; Mesenteries: Bi-k) polyps analyzed at 0, 24, 48 and 96 hours post-pulse (hpp). In A and B, nuclei are labeled with DAPI (cyan) and EdU retaining cells are recognized by their green staining. White arrows at 24hpp in uncut (Ab) and cut (Af) polyps indicate the appearance of EdU cell pairs. Green and orange double arrowheads in Ag indicate the accumulation of the EdU+ retaining cells at the amputation site of the regenerating polyp, and the EdU depleted zone, respectively. No accumulation of EdU+ retaining cells is detected in uncut animals (Aa-d). In B, the accumulation of EdU+ retaining cells in the most oral part of the mesenteries starts at 24hpa (Bj) and become stronger at 48hpa (Bk). The green double arrowhead and the discontinued line, in Bj and k, indicate the accumulation of the EdU+ retaining cells, in the epithelia and in the mesenteries, respectively. The orange double arrowhead in Bk indicates the EdU depleted zone in the mesenteries. *mes*, mesenteries.

Additional Files: Figure legends

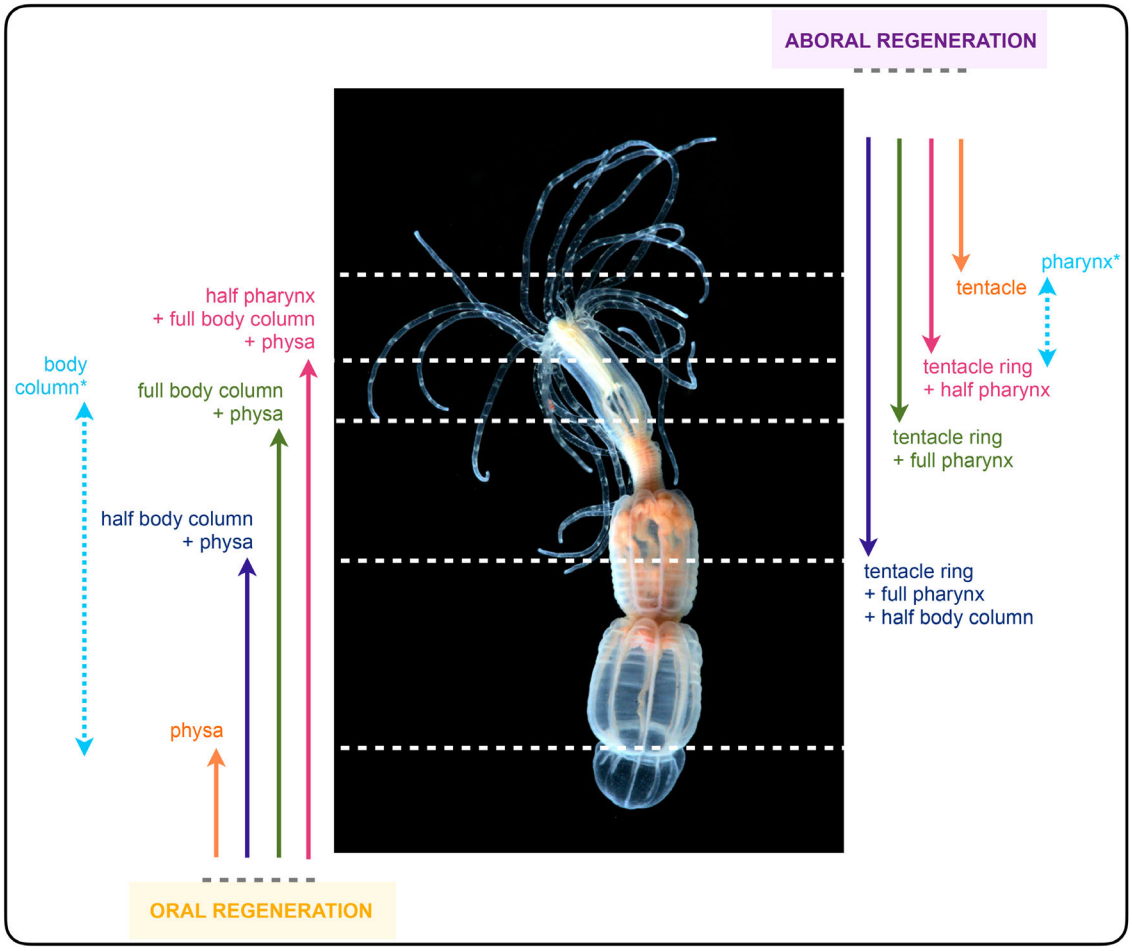

Figure S1. Diagram summarizing the various amputation sites along the body column of *Nematostella* used in this study. The asterisks for [body column] and [pharynx] indicate that in those isolated parts of the animal, oral and aboral regeneration were scored.

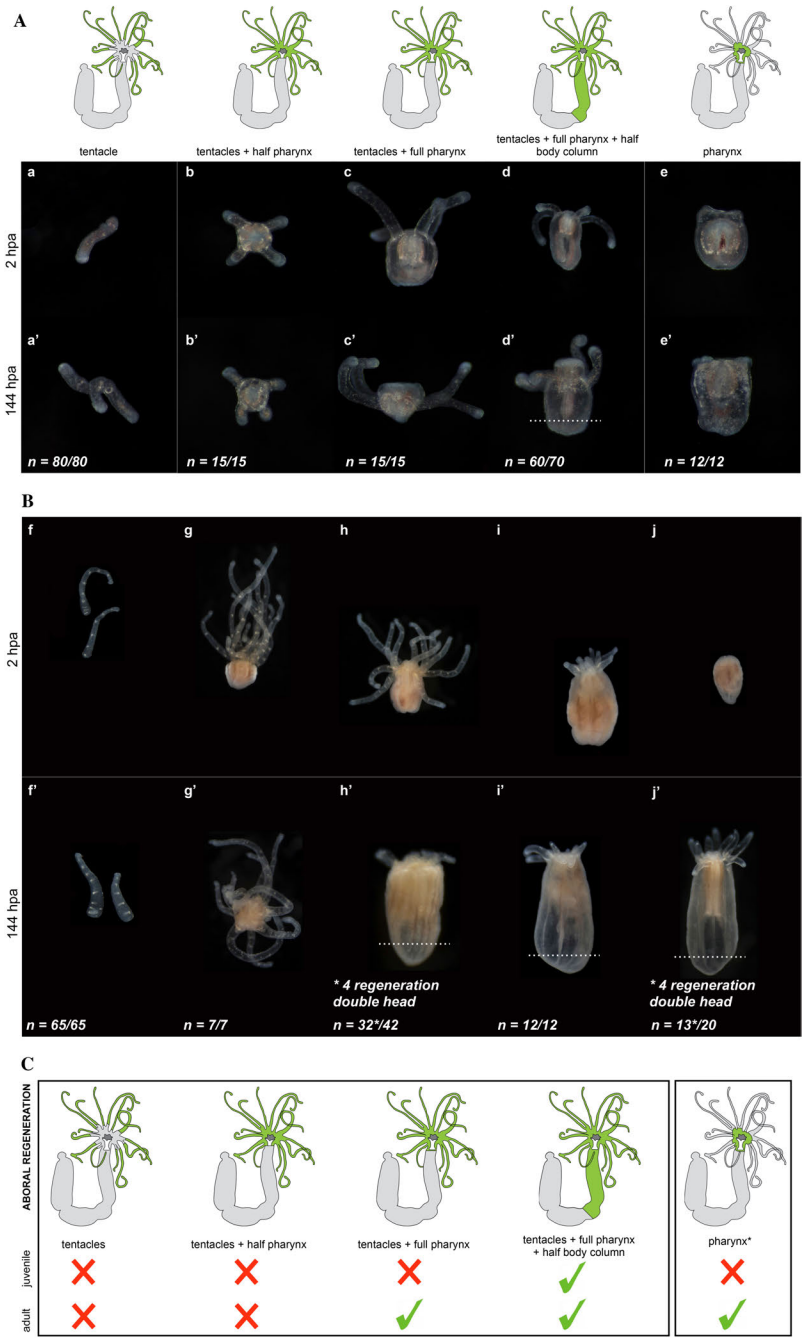

Figure S2. Aboral regenerative capacity analyzed in juveniles (Aa-e, Aa'-e') and in adults (Bf-j, Bf'-j') from isolated [tentacles] (Aa, Aa', Bf, Bf'); [tentacles + half pharynx] (Ab, Ab', Bg, Bg'); [tentacles + full pharynx] (Ac, Ac', Bh, Bh'); [tentacles + half pharynx + half body column] (Ad, Ad', Bi, Bi'); [pharynx] (Ae, Ae', Bj, Bj'). The success of aboral regeneration is indicated by the development of a new physa delimitated by the white dashed line. Photographs of the isolated body parts at 2hpa (Aa-e, Bf-j). Phenotypes observed after 144hpa (6 days post amputation) (Aa'-e', Bf'-j'). n=[number of specimen with represented phenotype]/[total number of analyzed specimen]. (*) indicates that from the pool of isolated body parts, four animals regenerated with two oral but no aboral regions. **C**. Diagram summarizing the aboral regeneration experiments carried out in juveniles and adults. Green parts in the schematic *Nematostella* indicate the isolated body part, green checkmarks the regenerative success and red crosses the absence of regeneration after body part isolation.

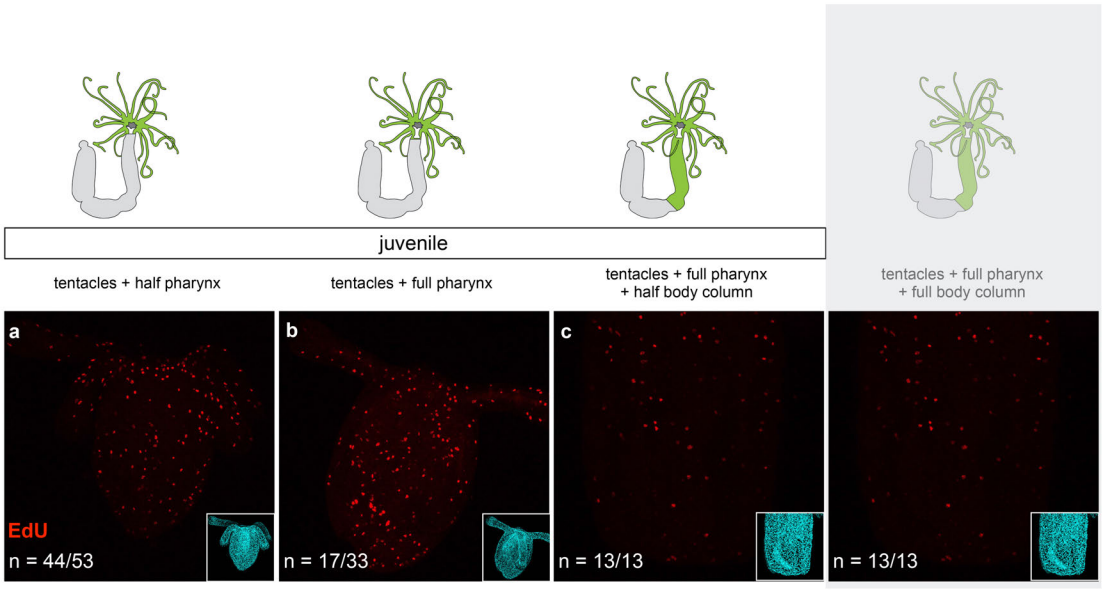

Figure S3. Cell proliferation at 48hpa in [tentacles + half pharynx] (a); [tentacles + full pharynx] (b); [tentacles + full pharynx + half body column] (c). Confocal microscopy images showing cellular proliferation (EdU labeling, a-c; red) and nuclei using DAPI (cyan, right bottom square) for corresponding images. n=[number of specimen with represented phenotype]/[total number of analyzed specimen].

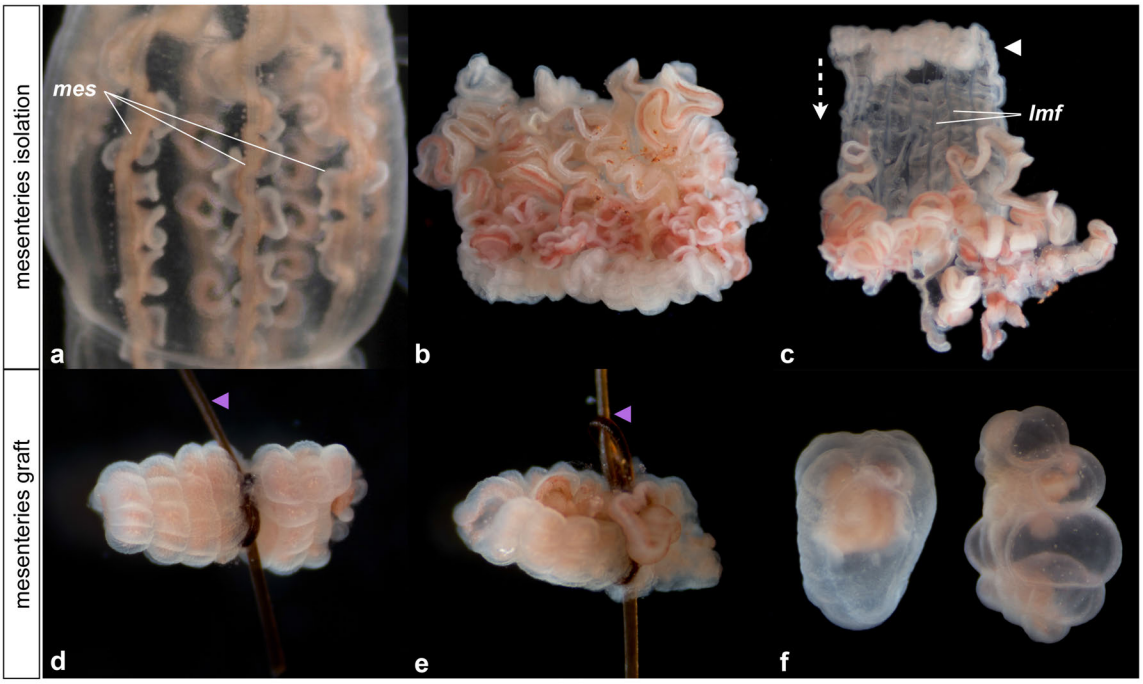

Figure S4. Macrophotographs illustrating the tissue isolation and grafting experiments. (a-c) are images of the experimental protocol for the isolation of the mesenteries and the body wall epithelia. (d, e) are images of the [mes] + [ecto + gastro] grafts immediately after the combination. Purple arrowheads indicate the organic string required to maintain the tissues together. (f) is an image of two samples three days after grafting the tissues together and in which the graft between the mesenteries and the body wall epithelia was successful (and later regenerated). Note that the integrity of the mesenterial tissue (pink) is maintained.

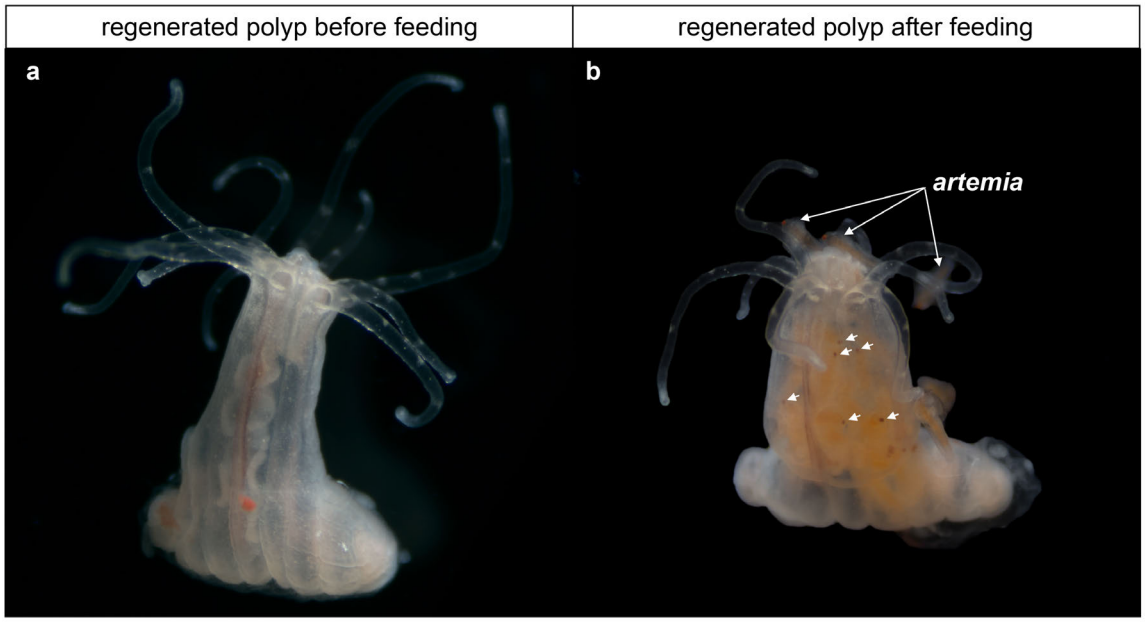

Figure S5. Macrophotographs illustrating regenerated polyps before feeding (a) and after feeding (b). The white arrows in (b) show the eaten artemia (brine shrimp).

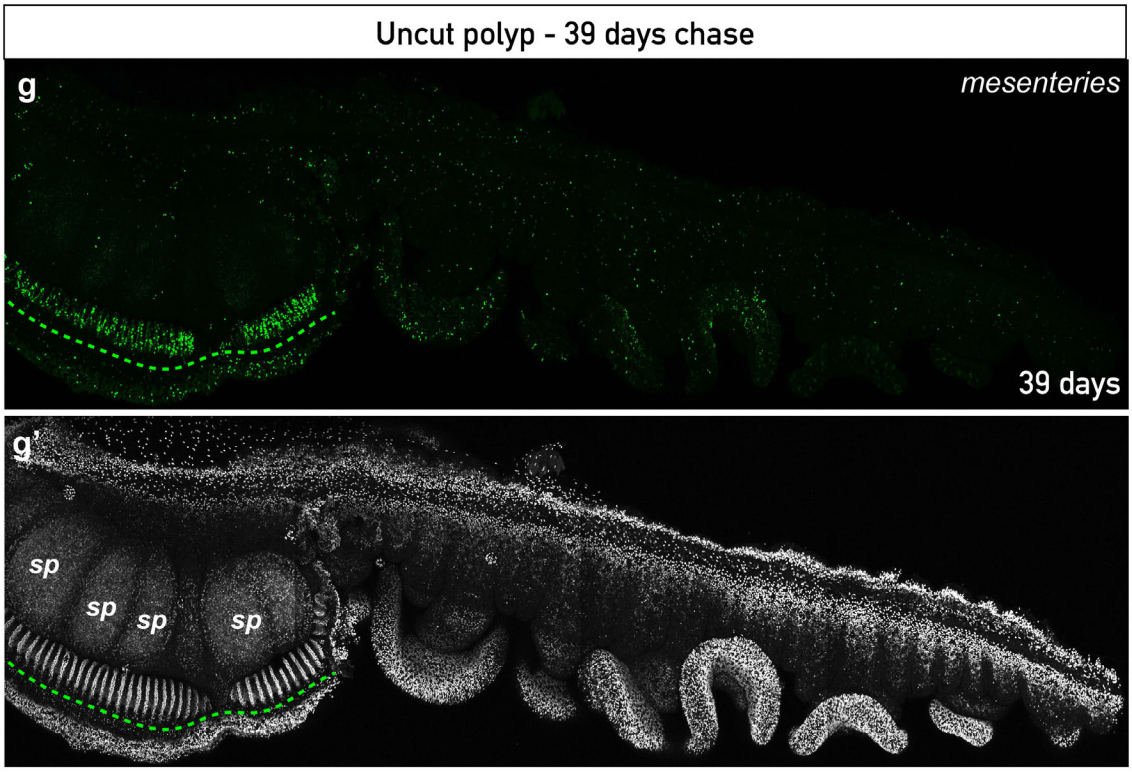

Figure S6. Presence of Label (EdU) Retaining cells (LRCs) in uncut adult gonads. The discontinued line (g,g') show the LRCs and the zone of LRCs accumulation in the gonad, respectively. LRC EdU staining in green (g) and DAPI staining that is labeling the nuclei in white (g'). *sp*, sperm mass.

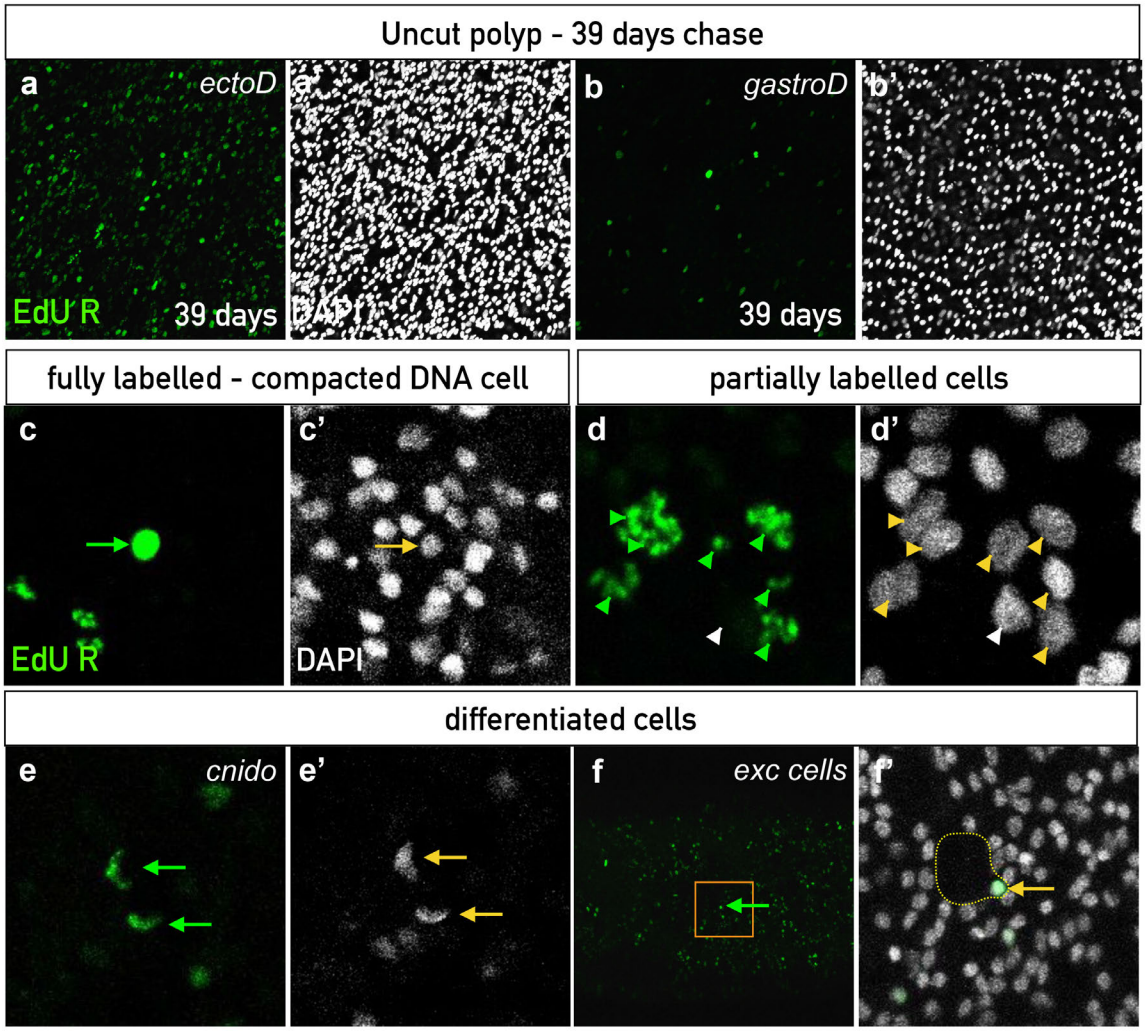

Figure S7. Presence of Label (EdU) Retaining cells (LRCs) in uncut adults. Confocal images of the LRCs in adult epithelia chased at 39 days (EdU R in green, a-e) after a one-week pulse. Nuclei are in white (DAPI) (a'-e'). Overlay of EdU and DAPI staining in d'. The renewal of the gastrodermal cells seems faster than the ectodermal cells as LRCs are more isolated and sparse in the gastrodermis than in the ectodermis in adults (a,b). Within the LRCs, one can distinguish differentiated cells such as cnidocytes (e,e'), excretory cells (f,f'; discontinued line in f') and batteries of nematocysts. The latter have partially labeled nuclei potentially because of their several rounds of cell division (d,d'). Cells with highly condensed DNA are also found (c,c'). Green arrows (c,e-f) and arrow heads (d) indicate the LRCs EdU staining. Yellow arrows (c',e'-f') and arrow heads (d') indcate the LRCs nuclei. Note that one cell of the batteries of the nematocysts is poorly or not labeled (white arrow head in d') probably due to the dilution of the signal through cell divisions. f' is a magnification of the square represented in f. *ectoD*, ectodermal view; *exc cells*, excretory cells; *gastroD*, gastrodermal view.

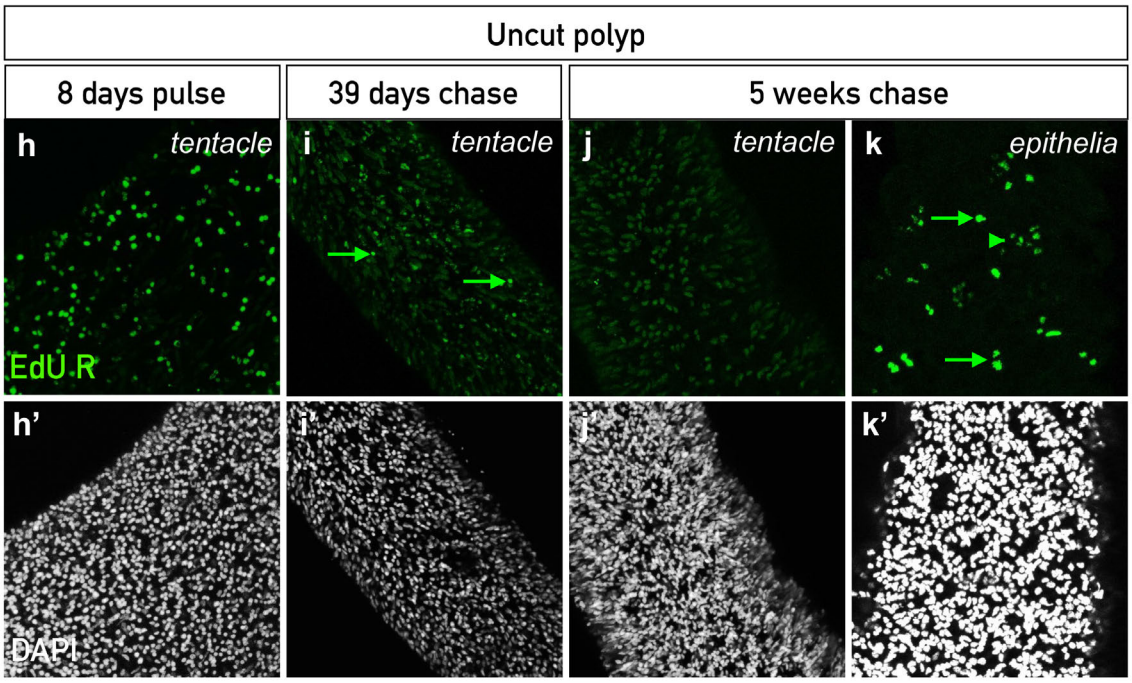

Figure S8. LRCs at 8 days after pulse (h), 39 days chase (i) and 5 months chase (j) in the tentacles of the uncut polyp. LRCs are present in the tentacles up to 39 days (i) but not at 5 months chase (i). However, they are still present in the body wall epithelia of the 5 months chase (k). LRC EdU staining in green (h-k) and DAPI staining labeling the nuclei in white (h'-k'). Green arrows (h,i,k) show the LRCs. Green arrowhead in k shows potential batteries of nematocysts.

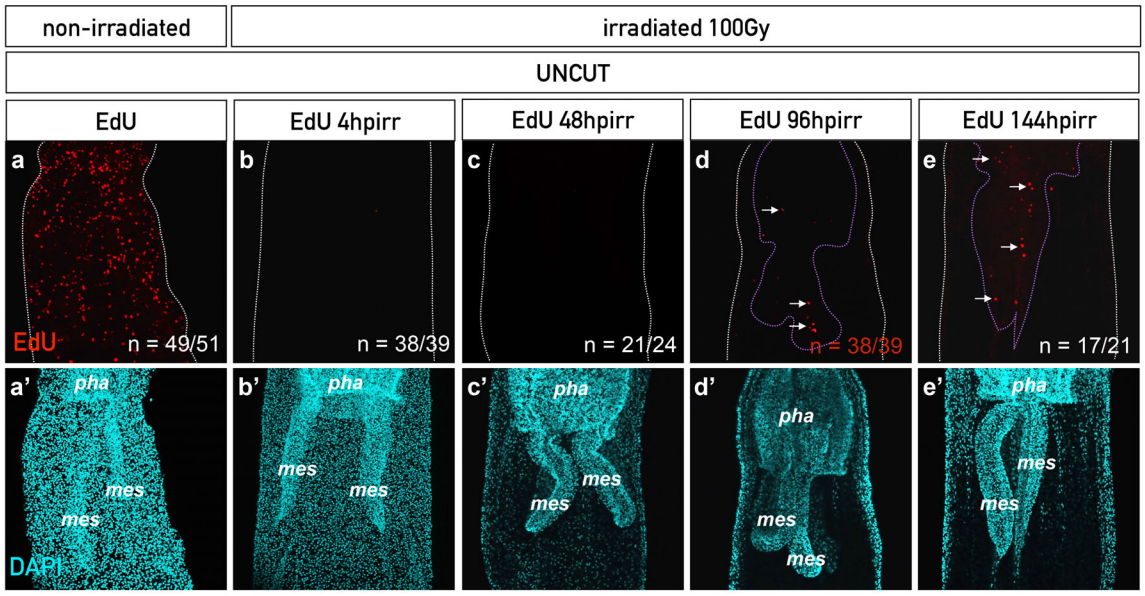

Figure S9. Irradiation blocks cell proliferation (a,a',b,b') and a population of cells is able to re-inter the mitotic cycle between 48 and 96 hours post irradiation (hpirr) in the uncut animal. Confocal images of control non irradiated (a,a') and irradiated (b-e,b'-e') uncut polyps. While cell proliferation is blocked after irradiation (a,a',b,b'), a few cells in the mesenteries, were able to re-enter the cell cycle between 48 and 96hpirr. They were also detectable at 144hpirr within the mesenteries and in the pharyngeal region (e,e'). *mes*, mesenteries; *pha*, pharynx. n=[number of specimen with represented phenotype]/[total number of analyzed specimen].

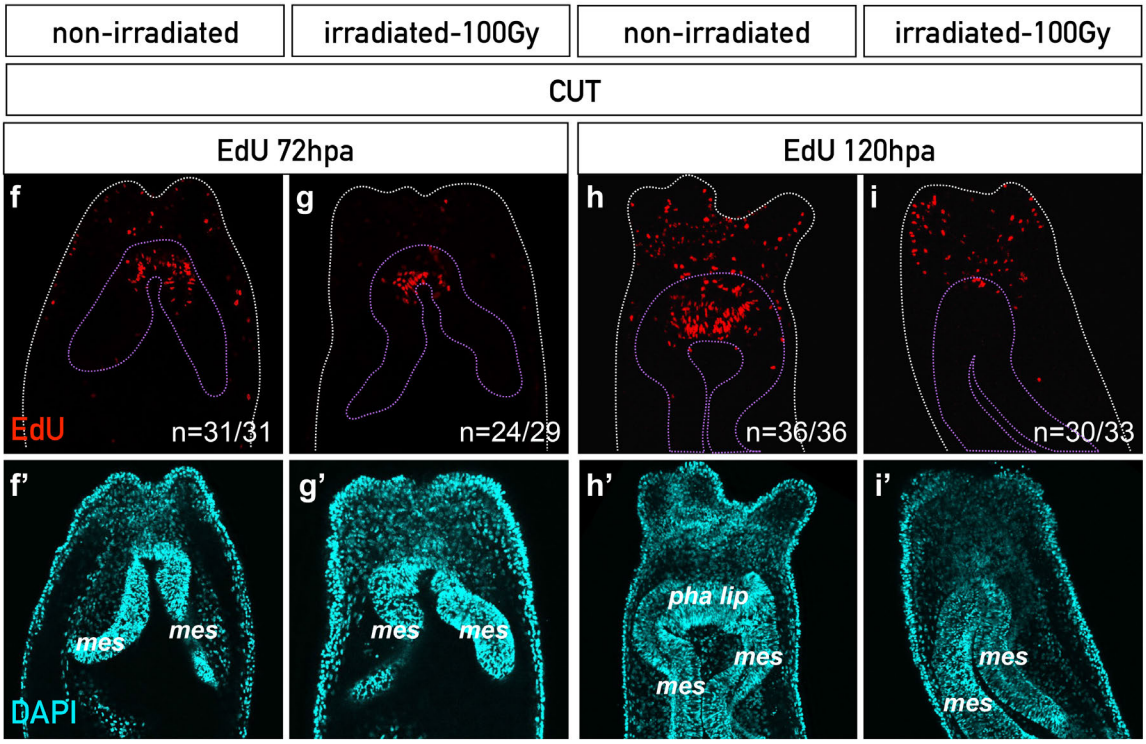

Figure S10. A population of cells is able to re-enter the mitotic cycle between 24 and 48 hours post amputation (hpa) (corresponding to 28 and 52hpirr) in the 100 Grays irradiated polyps. Confocal images of control non irradiated (f,f': 72hpa; h,h': 120hpa) and irradiated (g,g': 72hpa; i,i': 120hpa) polyps. The cells in the mesenteries, localized at the amputation site, that re-entered the cell cycle between 24 and 48hpa are also detectable at 72 and 120hpa (g,i). EdU staining in red shows cell proliferation (f,i). Nuclei are in cyan (DAPI) (f',i'). *mes*, mesenteries; *pha lip*, pharyngeal lip; *ten*, tentacles. n=[number of specimen with represented phenotype]/[total number of analyzed specimen].

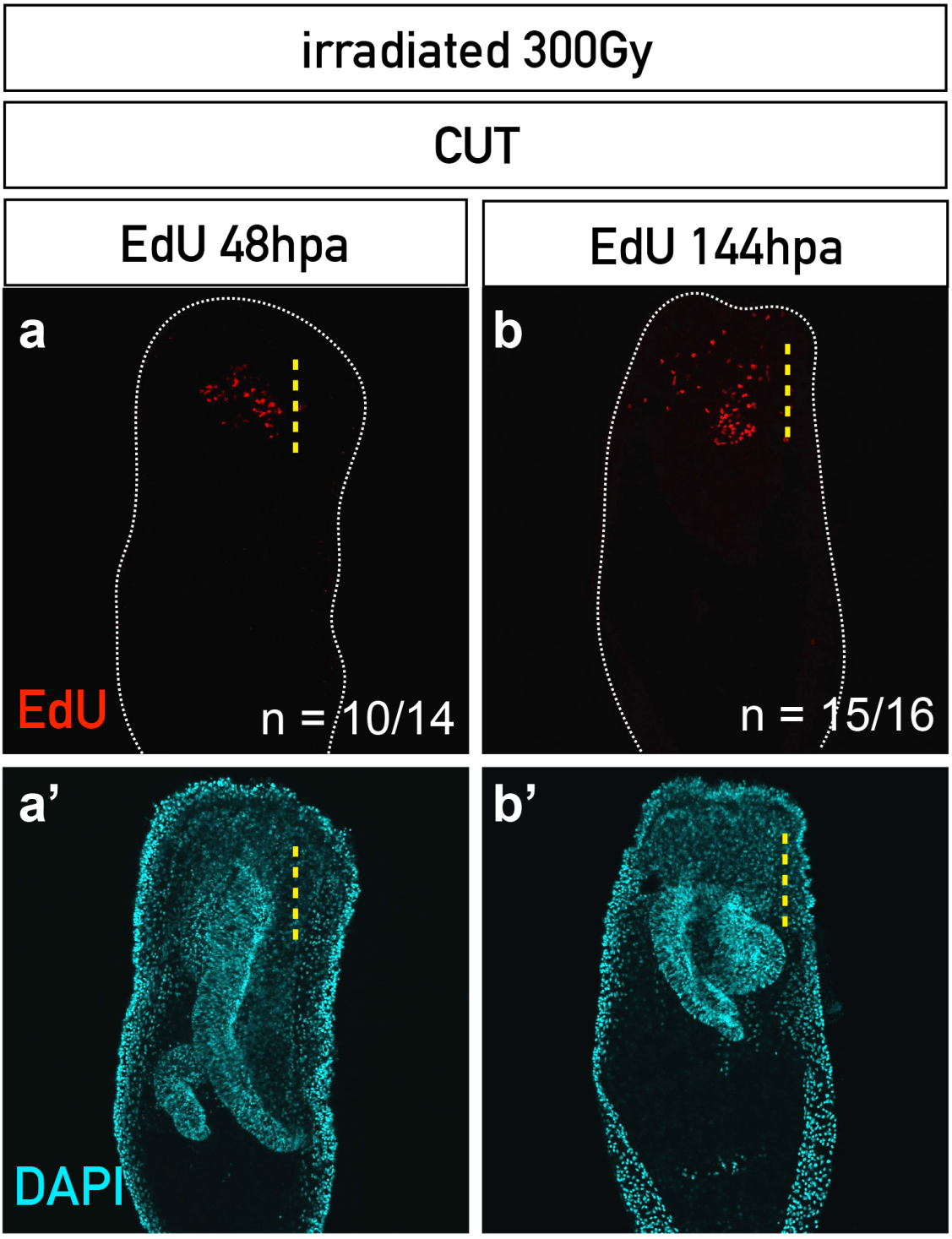

Figure S11. A population of cells is able to re-enter the mitotic cycle between 24 and 48 hours post amputation (hpa) (corresponding to 28 and 52hpirr) in 300 Grays irradiated polyps. Confocal images of irradiated and amputated polyp (j,j': 48hpa; k,k': 144hpa). EdU staining in red shows cell proliferation (j,k). Nuclei are in cyan (DAPI) (j',k'). *mes*, mesenteries. n=[number of specimen with represented phenotype]/[total number of analyzed specimen].

A	Step 0	Step1	Step2	Step3	Step4
non irradiated observed at 48hpa	2/15	5/15	**8/15**	0/15	0/15
irradiated 100 gray observed at 48hpa	3/16	6/16	**7/16**	0/16	0/16
irradiated 300 gray observed at 48hpa	2/14	**10/14**	2/14	0/14	0/14
non irradiated observed at 144hpa	0/38	0/38	3/38	9/38	**26/38**
irradiated 100 gray observed at 144hpa	1/31	7/31	**21/31**	2/31	0/31
irradiated 300 gray observed at 144hpa	0/16	1/16	**15/16**	0/16	0/16

B	Step 0	Step1	Step2	Step3	Step4
non irradiated observed at 24hpa	0/14	**14/14**	0/14	0/14	0/14
irradiated 100 gray observed at 24hpa	**10/19**	9/19	0/19	0/19	0/19
non irradiated observed at 48hpa	0/16	**14/16**	2/16	0/16	0/16
irradiated 100 gray observed at 48hpa	1/21	**10/21**	8/21	1/21	0/21
non irradiated observed at 72hpa	0/31	0/31	**20/31**	11/31	0/31
irradiated 100 gray observed at 72hpa	0/29	5/29	**24/29**	0/29	0/29
non irradiated observed at 120hpa	0/36	0/36	0/36	12/36	**24/36**
irradiated 100 gray observed at 120hpa	0/33	3/33	**29/33**	1/33	0/33

Figure S12. The resulting phenotype from non-irradiated *vs* irradiated uncut animals that were bisected and then scored for regeneration progression at various time points after amputation in two independent experiments (**A**: experiment batch 1 and **B**: experiment batch 2).

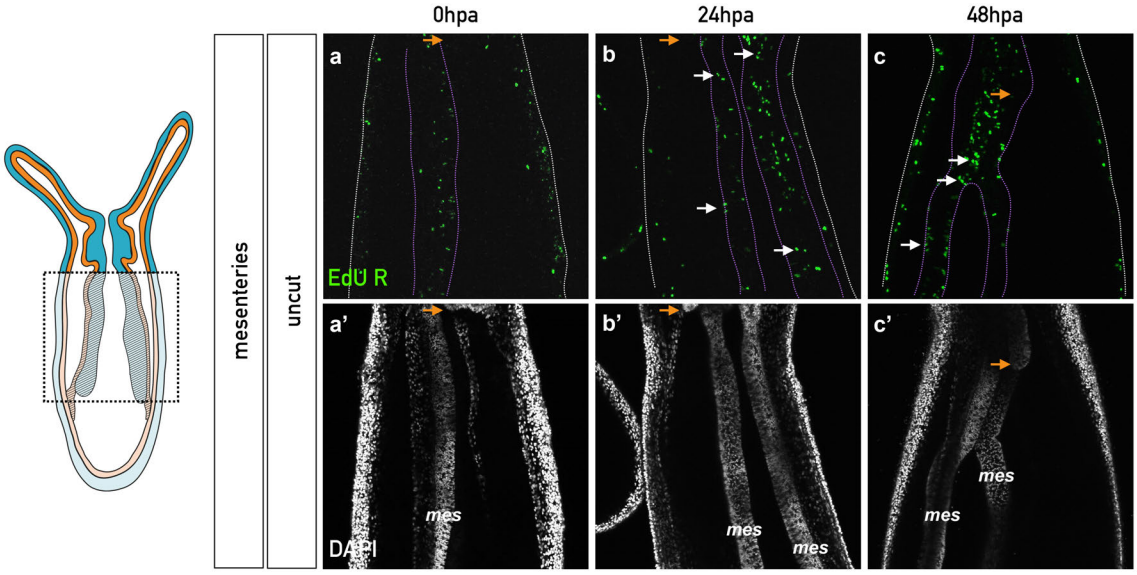

Figure S13. Chase of the EdU+ cells at 0, 24 and 48 hours post-1hour-pulse (hpp) in control uncut animals. Confocal images of EdU+ cells (EdU R) that are stained in green (a-c) and the nucleus in white (a'-c'). Orange arrows indicate the position of the pharynx. White arrows indicate EdU R cell pairs (b,c). No accumulation of EdU+ retaining cells is detected in uncut animals (Aa-d). The discontinued white and purple lines indicate the contours of the epithelia and mesenteries, respectively. *mes*, mesenteries.

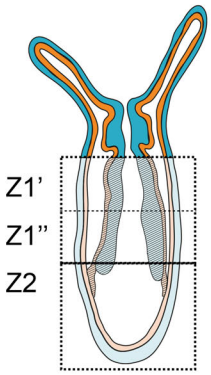

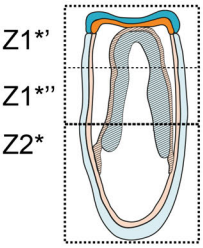

				0hpa	24hpa	48hpa	72hpa	96hpa	T
Body Epithelia	Uncut	Z1'	exp1	29	45	47	-	115	↑
			exp2	29	48	39	102	165	
			exp3	-	-	-	-	-	
		Z1''	exp1	44	48	47	-	138	↑
			exp2	43	49	41	86	141	
			exp3	-	-	-	-	-	
		Z2	exp1	71	108	111	-	206	↑
			exp2	70	94	102	158	213	
			exp3	-	-	-	-	-	
	Cut	Z1'*	exp1	23	45	129	-	368	↑↑↑
			exp2	26	42	133	219	371	
			exp3	-	43	136	225	363	
		Z1''*	exp1	41	39	69	-	63	-
			exp2	38	39	70	67	67	
			exp3	-	38	76	68	58	
		Z2*	exp1	60	78	145	-	70	↑↓
			exp2	59	81	150	123	120	
			exp3	-	80	160	126	129	

Figure S14. Average number of EdU R cells during the time course of regeneration in three different zones located along the oral-aboral axis of the body epithelia for uncut and cut (*) polyps. These zones are named Z1', Z1'' and Z2. All the described zones are restricted to the epithelia; mesenteries are excluded from the counting. The zones are defined as followed: Z1 - oral half of the polyp; Note that in the uncut animal, the region above the sub-pharyngeal line (the head) was not taken into account to define the zone; Z1' and Z1'' are the oral and aboral halves of Z1, respectively. Z2 - aboral half of the polyp. (*) is associated to the three zones defined in regenerating polyps (Z1'*, Z1''* and Z2*). Counting was performed in three independent experiments (*exp1*, *exp2*, *exp3*). Arrows on the right side indicate general variations of the average number of cells for the different zones in the uncut *vs* cut animals.